PART I

THE EFFECT OF SCREENS IN A WIDE ANGLE DIFFUSER OF SQUARE CROSS-SECTION

PART II

THE INFLUENCE OF THE PROXIMITY OF A WALL TO THE TEST SECTION EXIT OF A WIND TUNNEL

A THESIS

Presented to

the Faculty of the Graduate Division

Georgia Institue of Technology

In Partial Fulfillment

of the Requirements for the Degree

Master of Science in Aeronautical Engineering

By

Charles Lancaster Wharton, Jr.

June 1954

In presenting the dissertation as a partial fulfillment of the requirements for an advanced degree from the Georgia Institute of Technology, I agree that the Library of the Institution shall make it available for inspection and circulation in accordance with its regulations governing materials of this type. I agree that permission to copy from, or to publish from, this dissertation may be granted by the professor under whose direction it was written, or, in his absence, by the Dean of the Graduate Division when such copying or publication is solely for scholarly purposes and does not involve potential financial gain. It is understood that any copying from, or publication of, this dissertation which involves potential financial gain will not be allowed without written permission.

_____

_____

PART I

THE EFFECT OF SCREENS IN

A WIDE ANGLE DIFFUSER OF SQUARE CROSS-SECTION

PART II

THE INFLUENCE OF THE

PROXIMITY OF A WALL TO THE TEST SECTION EXIT

OF A WIND TUNNEL

Approved:

Date Approved by Chairman: May 31, 1954

ACKNOWLEDGEMENTS

The author wishes to express his appreciation to Dr. A. L. Ducoffe for his generous aid, valuable criticism, and guidance in the development and preparation of this thesis. The author is also indebted to Professor D. W. Dutton and the entire Aeronautical Engineering staff at the Georgia Institute of Technology for their valuable assistance and financial aid, without which this thesis could not have been completed. Gratitude is extended to Professors J. J. Harper and M. R. Carstens for their review and criticism of the topic.

PART I

THE EFFECT OF SCREENS IN A WIDE ANGLE DIFFUSER OF SQUARE CROSS-SECTION

LIST OF SYMBOLS

A	cross-sectional area of diffuser
d	wire diameter
d_1	equivalent entrance diameter of conical diffuser
d_2	equivalent exit diameter of conical diffuser
E	efficiency of diffuser or diffuser screen combination
H	total head pressure
K	pressure drop coefficient of screens
L	diffuser length
M	mesh per inch
p	static pressure
p_{at}	atmospheric pressure
Δp	change in static pressure between two points or across a screen
q	dynamic pressure
RN	Reynolds Number
S	solidity of screen, defined as closed area per inch
V	velocity
Y	diffuser width or height measured perpendicular to horizontal centerline
α	equivalent conical diffusion angle
β	wall angle of square diffuser
μ	fluid viscosity
ρ	fluid density

Subscripts 0, 1, 2, - - - n refer to positions along the axis of the diffuser, 0 at the diffuser entrance.

TABLE OF CONTENTS

TABLE OF CONTENTS (CONTINUED)

LIST OF TABLES

LIST OF ILLUSTRATIONS

PART I

LIST OF ILLUSTRATIONS (CONTINUED)

PART I

PART II

SUMMARY

The purpose of this part of the paper is to present the results of an investigation of the filling effect of fine mesh screen wire in a wide angle diffuser.

An Eiffel type wind tunnel containing a square diffuser with an equivalent conical diffusion angle of eighty-three degrees was designed and constructed. Two sets of fine mesh screens of twenty mesh per inch and thirty mesh per inch were tested in the diffuser at three different airspeeds ranging from twenty to seventy feet per second. Results of the investigation indicate that both sets of screens will satisfactorily fill the diffuser. The twenty mesh per inch set were found to be more practical because of the affinity of the screens for dust. Tuft studies indicate that the diffuser is filled for both sets of screens over the range of velocities tested.

CHAPTER I

INTRODUCTION

One of the most difficult problems in low speed aerodynamics in the past two decades has been the study of turbulence phenomena. From the outset, very little progress of an analytical nature was made because of the complexity of the mathematics. Therefore, experimental techniques were introduced. These techniques resulted in the development of the low turbulence wind tunnel along with refinements to the hot-wire anemometer which is the most satisfactory type of instrumentation for measuring turbulent fluctuations.

In order to produce an airflow with a low turbulence intensity, damping screens must be incorporated into the design of the wind tunnel. This is one of the design features which differentiates an ordinary low speed tunnel from a low turbulence tunnel. From the standpoint of efficiency, the screens must be located at a position in the tunnel where the velocity is a minimum, since the pressure loss through a screen is proportional to the velocity (at the screen) squared. Another design feature of a low turbulence tunnel is a large contraction ratio between the settling chamber and the working section. As a result, the tunnel must be designed with a very long diffuser with an equivalent conical diffusion angle of less than seven degrees, or a short, wide angle diffuser fitted with fine mesh screens to prevent separation. On the basis of construction costs, the latter scheme is the most desirable. However, the power requirements are considerable larger.

The most significant study on wide angle diffusers was made by Schubauer and Spangenburg, Ref. (1). The work in Ref. (1) presents an analytical and experimental study on wide angle diffusers with circular cross-section, incorporating several screen combinations for the prevention of flow separation.

The use of the wide angle diffuser in the design of the low turbulence tunnel at Georgia Tech is dictated by space limitations and limited funds. The purpose of this paper is to present an analytical and experimental study of the characteristics of a wide angle diffuser of square cross-section with two different screen combinations. The results of these tests are to be used as criteria for the design of the wide angle diffuser for the Georgia Tech low turbulence wind tunnel.

CHAPTER II

EQUIPMENT

The experimental work was carried out in an Eiffel type tunnel which is shown schematically in Fig. 1. The tunnel was designed to operate at a maximum velocity of one hundred feet per second at the entrance to the diffuser, station (86.3) Fig. 1.

A bell-mouth, station (0) Fig. 1 was placed on the intake end of the tunnel to facilitate the airflow into the entrance duct. A honeycomb, immediately downstream of the bell-mouth, was used to remove as many flow irregularities as possible. The honeycomb was constructed of one-eighth inch thick aluminum plate and had a fineness ratio of four to one.

The entrance duct, station (4.0) to station (86.3) Fig. 1 was square, in cross-section, with a constant area of eighty-nine square inches. The duct was eighty-two inches long and was constructed in three twenty-four inch sections, and one ten inch section. Each of the sections were constructed with three sides of plywood and the fourth side of plexiglass. The plexiglass side provided for visual observation of the flow in the duct.

The wide angle diffuser, station (86.3) to station (100.9) Fig. 1, was square in cross-section and had an equivalent conical diffusion angle of eighty-three degrees. An equivalent conical diffuser is defined as a diffuser, circular in cross-section, with the same entrance

and exit areas and the same length as the square diffuser. The entrance area was eighty-nine square inches and the exit area was six hundred-seventy six square inches, giving an area ratio of 7.6 to 1.

The exit duct, station (100.9) to station (220.9) Fig. 1, constructed in four, thirty inch sections, was one hundred twenty inches long and had a constant cross-sectional area of six hundred seventy-six square inches.

A sheet metal transition section, forty-eight inches long, was attached at station (220.9) Fig. 1. This duct was necessary to provide a change in tunnel cross-sectional area from six hundred seventy-six to two hundred fifty-four square inches and from square to circular in shape.

The power section, station (268.9) to station (315.40) Fig. 1, consisted of two circular aluminum alloy ducts forty-six inches in total length. A magnesium casting, which housed the rotor, was mounted between the two aluminum ducts. A gear box with a four to one ratio was attached to the casting and extended upstream from the casting. The gear box was covered with a streamlined fairing which constricted the airflow to the area swept by the rotor blades. The rotor consisted of a dural disk fourteen inches in diameter with thirty-six blades equally spaced around the periphery. The blades were two inches long and machined from aluminum alloy in the form of an R.A.F. - 6 airfoil section. The duct area at the rotor blades was one hundred one square inches. The blades were set at a blade angle of seventeen and one-half degrees. A conical diffuser extended downstream from the rotor. Fig. 2 is a photograph of the tunnel.

The power for the rotor was supplied by a fifteen horsepower electric motor coupled to a variable speed head, Fig. 3. The vari-drive head consisted of two shafts, one with a speed range of twelve hundred to fifty-five hundred RPM, and the other from five thousand to twelve thousand RPM. The lower speed shaft was used.

The drive unit was coupled to the gear box through a shaft with a universal joint mounted on each end. With this configuration the rotor speed range was from forty-eight hundred to twenty thousand RPM.

A bell-mouth was located at station (315.4) Fig. 1 to partly facilitate the diffusion of the flow, Fig. 4.

In order to provide velocities less than the minimum available with the vari-drive unit operating at twelve hundred RPM, an adjustable bleed was installed to allow air to enter the tunnel downstream of the diffuser, thereby permitting a lower velocity in the diffuser.

CHAPTER III

INSTRUMENTATION

In order to obtain static and total head pressure readings at various locations in the tunnel, six rakes of total head and static pressure tubes were constructed and installed on the vertical centerline of the tunnel as shown in Fig. 1.

Because of the difficulty of construction and operation of probes between the screens, static pressure tubes were mounted in rear side wall of the diffuser on the horizontal centerline. Twenty-six flush wall orifices were installed in order to read the static pressure in front of, behind, and between each of the screens, Fig. 5.

The pressure tubes from the six rakes and those from the diffuser were connected to a manifold, Fig. 6. By using sheet metal pinch clamps, any single tube or combination of tubes could be read on a single manometer.

A piezometer ring was constructed and installed to measure the static pressure rise across the diffuser, and a second piezometer ring was installed at the rotor to measure the static pressure rise across the rotor blades.

The speed of the rotor was controlled by the vari-drive unit by means of a tachometer mounted on the vari-drive instrument panel, and the velocity of the air flow at the diffuser entrance was controlled by the combination of the rotor speed and the bleed position.

Tufts were installed on the screens in the diffuser and at the

entrance and exit of the diffuser to provide visual means for determining separation of the flow in the diffuser.

CHAPTER IV

PROCEDURE

Because of the variation in blocking effect caused by the different combinations of screens, the calibration made for one set of screens would not necessarily be true for another set. For this reason each set of screens was tested at the same bleed positions, rotor speeds, and power settings. This procedure necessarily provided slightly different airspeeds for the two sets of screens. Each set of screens was tested at three different airspeeds corresponding to different combinations of rotor speed and bleed position. The static and total head pressures were measured at rakes II and III, located upstream and downstream respectively, of the wide angle diffuser. The static pressures between the screens were measured at each of the tube locations on the wall of the diffuser. The average static pressure change across the diffuser and across the rotor blade was also measured. During these tests tuft studies were made in the diffuser region to determine whether any separation of the flow occurred, the amount of separation, and the possible cause of separation.

CHAPTER V

DIFFUSER DESIGN

As stated in Ref. (1) the efficiency of the diffuser is defined as

$$E = \frac{\text{gain in potential energy}}{\text{loss in kinetic energy}} \tag{1}$$

Considering the efficiency in stages for multiple screens, let $E_{0,1}$ be the efficiency from section 0 to the downstream side of screen 1, $E_{1,2}$ be the efficiency from the downstream side of screen 1 to the downstream side of screen 2, and so on. Then according to equation (1),

$$E_{0,1} = \frac{p_1 - p_0}{q_0 - q_1} \tag{2}$$

$$E_{1,2} = \frac{p_2 - p_1}{q_1 - q_2}$$

where, p_1 and q_1 are the integrated static and dynamic pressures at station 1. Subscript "0" refers to the diffuser entrance, subscript "1" refers to a position immediately downstream of screen number 1, and so on. Since the overall efficiency is

$$E_{0,n} = \frac{p_n - p_0}{q_0 - q_n} \tag{3}$$

it follows by substitution and rearrangement that

$$E_{0,n} = E_{0,1} \frac{1 - \frac{q_1}{q_0}}{1 - \frac{q_n}{q_0}} + E_{1,2} \frac{\frac{q_1}{q_0} - \frac{q_2}{q_0}}{1 - \frac{q_n}{q_0}} + - - - \qquad (4)$$

It follows from equation (4) and by assuming the flow efficiency is unity that

$$E_{0,1} = 1 - \frac{\Delta p_1}{q_0 - q_1}$$

$$E_{1,2} = 1 - \frac{\Delta p_2}{q_1 - q_2} \qquad (5)$$

where Δp_1 , Δp_2 and so forth are the pressure drops across screens 1 and 2 respectively, and the flow efficiency is defined as the efficiency not including the losses due to the screens themselves. It follows from definition that

$$\Delta p_1 = K_1 \, q_1$$

$$\Delta p_2 = K_2 \, q_2$$

where K_1 , K_2 - - - are the loss coefficients of screens 1, 2, etc., and q_1 , q_2, etc. are the dynamic pressures at screens 1, 2 from which

$$E_{0,1} = 1 - \frac{K_1}{\frac{q_0}{q_1} - 1}$$

$$E_{1,2} = 1 - \frac{K_2}{\frac{q_1}{q_2} - 1} \qquad (6)$$

If the q's are uniform over each section, their ratio's may be expressed in terms of the area ratios, and equations (4) and (6) become,

$$E_{0,n} = E_{0,1}\frac{1-\left(\frac{A_0}{A_1}\right)^2}{1-\left(\frac{A_0}{A_n}\right)^2} + E_{1,2}\frac{\left(\frac{A_0}{A_1}\right)^2-\left(\frac{A_0}{A_2}\right)^2}{1-\left(\frac{A_0}{A_n}\right)^2} + - - \quad (7)$$

$$E_{0,1} = 1 - \frac{K_1}{\left(\frac{A_1}{A_0}\right)^2 - 1}$$

$$E_{1,2} = 1 - \frac{K_2}{\left(\frac{A_2}{A_1}\right)^2 - 1} \quad (8)$$

where A_0, A_1, A_2, - - - are the areas at stations 0, 1, 2, - - respectively. By designing for an overall efficiency of zero and a flow efficiency of unity where the overall efficiency of zero is assumed on the basis of no change in static pressure between the entrance and exit of the diffuser as the rise in static pressure due to increasing area is offset by the drop across each of the screens, and the flow efficiency is assumed to be one on the basis that the eddy losses due to the screens and the wall losses may be neglected at the low velocities. A more realistic value of the flow efficiency is 0.9, the following relations for the cross-sectional areas in which the screens are to be

placed may be obtained from equation (8) as

$$\frac{A_1}{A_0} = (K_1 - 1)^{1/2}$$
$$\frac{A_2}{A_1} = (K_2 - 1)^{1/2} \qquad (9)$$

For the overall area ratio

$$\frac{A_n}{A_0} = (K_1 + 1)^{1/2} \quad (K_2 + 1)^{1/2} \text{ - - - - } (K_n + 1)^{1/2} \qquad (10)$$

and if the K's for all screens are identical, equation (10) reduces to

$$\frac{A_n}{A_0} = (K + 1)^{n/2}$$

which states that, since the area ratio of the diffuser is specified, the number of screens necessary to attain zero efficiency is fixed by K.

The diffuser tested in these experiments was a scale model of the diffuser to be used in the Georgia Tech low turbulence wind tunnel. The dimensions of the Georgia Tech low turbulence tunnel diffuser, which were dictated because of space limitations, are as follows:

Equivalent entrance diameter	4.5 Ft.
Entrance area	15.92 Ft.^{2}
Exit area	121 Ft.^{2}
Equivalent exit diameter	12.4 Ft.
Diffuser length	4.5 Ft.

Equivalent conical diffusion angle, α , Fig. 7.

$$1/2\ \alpha = \tan^{-1} \frac{6.2 - 2.25}{4.5} = 41.5^\circ$$

or $\alpha = 83^\circ$

$$\text{Area ratio} = \frac{\text{Exit area}}{\text{Entrance area}} = \frac{121}{15.92} = 7.6$$

Using the same area ratio and equivalent conical diffusion angle, the dimensions of the scale model diffuser were established, Fig. 8.

Entrance area	89 in.^{2}
Equivalent entrance diameter, d_1,	10.66 in.
Exit area, (89 x 7.6)	676 in.^{2}
Equivalent exit diameter, d_2,	29.25 in.
Diffuser length, L,	

$$L = \frac{\frac{d_2}{2} - \frac{d_1}{2}}{\tan \alpha} \qquad 10.46 \text{ in.}$$

Since the diffuser was square in cross-section the wall angles will be different from the equivalent conical diffusion angle of eighty-three degrees. The wall angle to give the equivalent conical diffusion angle of eighty-three degrees was found as follows:

Entrance dimensions = $\sqrt{89} = 9.43$

Exit dimensions = $\sqrt{676} = 26$

wall angle, β

$$\tan \beta = \frac{26 - 9.43}{2 \times 10.46} = 0.792$$

$$\beta = 38.5^\circ$$

The dimensions for the basic diffuser are shown in Figs. 7 and 8. When the diffuser was designed, a twelve inch radius was superimposed on the entrance section of the diffuser in order to offer a smooth transition to the flow for the expansion process, Fig. 5. No radius was deemed necessary at the exit because of the low velocity at this station.

The locations of the screens were determined by use of equation (9) and the continuity equation. The Reynolds Number was computed on the basis of the wire diameter by the equation,

$$RN = \frac{\rho}{\mu} V d \qquad (11)$$

where

ρ = fluid density

V = velocity

d = wire diameter

μ = fluid viscosity

For the two different sets of screens tested the Reynolds Number and solidity, (defined as the closed area per inch) are as follows:

Mesh	diameter	R.N.	Open area per inch	Closed area per inch
20	.0090	4.788V	.6724	.3276
30	.0065	3.458V	.6480	.3520

The screen loss coefficient, K, which was plotted from references (1), (2), and (3), was read from Fig. 9. The solidity, or closed area per inch, was calculated from

$$S = 1 - (1 - dM)^2 \qquad (12)$$

where

S = solidity

d = wire diameter

M = mesh per inch

An iterative procedure was necessary to locate the screen positions. The calculations are shown in Table 1 with the method of computation being described as follows. The design entrance velocity was 57.7 feet per second. With this velocity the Reynolds Number at the first screen was approximated by RN = (4.788) (57.7) for the twenty mesh screen and RN = (3.458) (57.7) for the thirty mesh screen. Knowing the Reynolds Number and the closed area per inch of the screen, the loss coefficient was read from Fig. 9. The curves in Fig. 9 were extrapolated to provide loss coefficients in the lower Reynolds Number range. Since the losses in the lower Reynolds Number range were a small percentage of the total loss the extrapolation was not felt to be critical. With the loss coefficient, the area ratio between the entrance and the first screen was calculated by use of equation (9). Then knowing the entrance area, the area at the first screen was found. Using the continuity equation, $A_0 V_0 = A_1 V_1$, the velocity at the first screen was found. With a new Reynolds Number based on the new velocity the process was repeated to give a closer approximation to the correct area ratio. Since the process converged quite rapidly, only two iterations were required for each screen location. This procedure was continued until the full length of the diffuser had been traversed. The last screen, located at the exit of the diffuser is a 20 by 20 mesh screen (for both sets of

screens) and could actually have been placed at a larger area ratio since it provided more than the necessary pressure drop in both cases. However, the velocity through this last screen is so small that the pressure drop is negligible (approximately 2 per cent of the total drop). Thus, having the areas in the diffuser at which the screens were to be placed, the locations from the diffuser entrance were calculated.

CHAPTER VI

RESULTS

The results of this investigation are shown in Figs. 10 through 25. In Figs. 10 and 14 the static, total head, and dynamic pressure distributions at rake II are shown. The average values of the dynamic pressure were obtained by integration of the dynamic pressure distributions shown. Figs. 11, 12, 15, and 16 show the static, total head, and dynamic pressure distributions at rake III. The uniform distribution of the dynamic pressure downstream of the diffuser is evident in Figs. 12 and 16. In Figs. 13 and 17 the static pressure distribution in the diffuser is plotted. Also shown in these figures are the screen locations measured downstream from the diffuser entrance on the horizontal centerline. Figs. 18 and 22 show the tufts in the diffuser at zero velocity with the plexiglass side removed for the twenty and thirty mesh screens respectively. Tuft studies at an airspeed of approximately 52 feet per second are shown in Figs. 19 through 21 for the twenty mesh screens, and Figs. 23 through 25 for the thirty mesh set. Figs. 19 and 23 show a tuft grid at the entrance to the diffuser. The slight fluctuations of the tufts in these figures are attributed to the vortices set up in the flow by the wires on which the tufts were mounted. It will be noticed that the tuft mounted at the point where the wires cross is fluctuating more violently than any other because it encounters vortices set up by both wires. Figs. 20 and 24 show the tufts in the diffuser. Inspection of

this figure shows a slight amount of separation in the corner of the diffuser. This separation could be traced directly to leakage of air into the diffuser around the screen frames and was corrected during the runs in which the pressure measurements were taken. Figs. 21 and 25 show a tuft grid at the exit of the diffuser. In this figure it will be noticed that separation exists in the vicinity of the horizontal center-line tufts, on the near side. This separation is attributed to leakage around the screen frames on the plexiglass side of the diffuser, as the tufts symmetrically located on the back side did not show separation. Photographs of the tufts were taken at other speeds but the effect of speed on the tufts was negligible.

CHAPTER VII

CONCLUSIONS

1. From pressure measurements it appears that the loss in power due to the blocking effect of the screens will be less using the twenty mesh screens.

2. From a practical standpoint the twenty mesh screens should be used in preference to the thirty mesh set because of the affinity of the higher mesh screens for dust.

3. When fine mesh screens are used in a diffuser such as the one tested, the velocity distribution downstream appears to be adequately uniform except in the corners where secondary flows are present.

CHAPTER VIII

RECOMMENDATIONS

1. Further studies of the flow in the diffuser should be undertaken using more adequate instrumentation in the diffuser. If possible instruments should be designed to record the pressure distributions across the diffuser between the screens.

2. A filter should be placed on the intake end of the tunnel to remove as much dust as possible from the airflow to prevent the dust from collecting on the screens.

3. A method for providing known turbulence in the airstream at the diffuser entrance should be incorporated and the reduction in turbulence through the diffuser should be measured.

4. A hot-wire anemometer should be used to measure the turbulence at the diffuser exit in order to evaluate the turbulence damping effect of screens used to fill a wide angle diffuser.

Table 1. Theoretical calculation of Screen Locations

Vel.	RN	K	$\frac{A_{n+1}}{A_n}$	A_{n+1}	Vel.	RN	K	$\frac{A_{n+1}}{A_n}$	A_{n+1}	Y_n	$\frac{Y_n}{2}$	Vel.	Screen #	q	$\frac{\Delta p}{q}$ xq
								20 Mesh							
57.70	276	0.670	1.292	115.0	44.60	213.0	0.700	1.305	116.0	10.78	5.390	44.30	1	2.3300	1.632
44.30	211	0.700	1.305	151.5	33.90	162.0	0.740	1.320	153.0	12.38	6.190	33.60	2	1.3500	1.000
33.60	161	0.740	1.320	202.0	25.40	121.5	0.800	1.341	205.0	14.32	7.160	25.05	3	0.7460	0.597
25.05	120	0.800	1.341	275.0	19.00	91.0	0.860	1.365	280.0	16.75	8.380	18.35	4	0.4000	0.344
18.35	88	0.870	1.370	383.0	13.40	64.0	0.950	1.395	391.0	19.60	9.800	13.10	5	0.2040	0.194
13.10	63	0.960	1.400	547.0	9.36	45.0	1.040	1.430	560.0	23.65	11.825	9.15	6	0.0995	0.103
9.15	---	---	1.206	676.0	7.56	36.0	1.120	1.452	676.0	26.00	13.000	7.56	7	0.0680	0.076
															3.946
								30 Mesh							
57.70	199	0.750	1.325	118.0	43.60	151.0	0.795	1.340	119.0	10.90	5.450	43.20	1	2.2150	1.760
43.20	149	0.800	1.342	160.0	32.10	111.0	0.860	1.365	162.5	12.75	6.375	31.60	2	1.1890	1.020
31.60	109	0.860	1.365	222.0	23.80	80.0	0.940	1.393	226.0	15.05	7.525	22.70	3	0.6125	0.576
22.70	78	0.945	1.397	316.0	16.75	56.0	1.050	1.430	324.0	18.00	9.000	15.80	4	0.2960	0.311
*15.80	54	1.060	1.435	465.0	11.00	38.0	1.160	1.470	476.0	21.82	10.910	10.75	5	0.1370	0.159
*10.75	51	1.010	1.420	676.0	7.58	36.0	1.120	1.451	676.0	26.00	13.000	7.40	6	0.1060	0.119
															3.945

*20 Mesh Screen

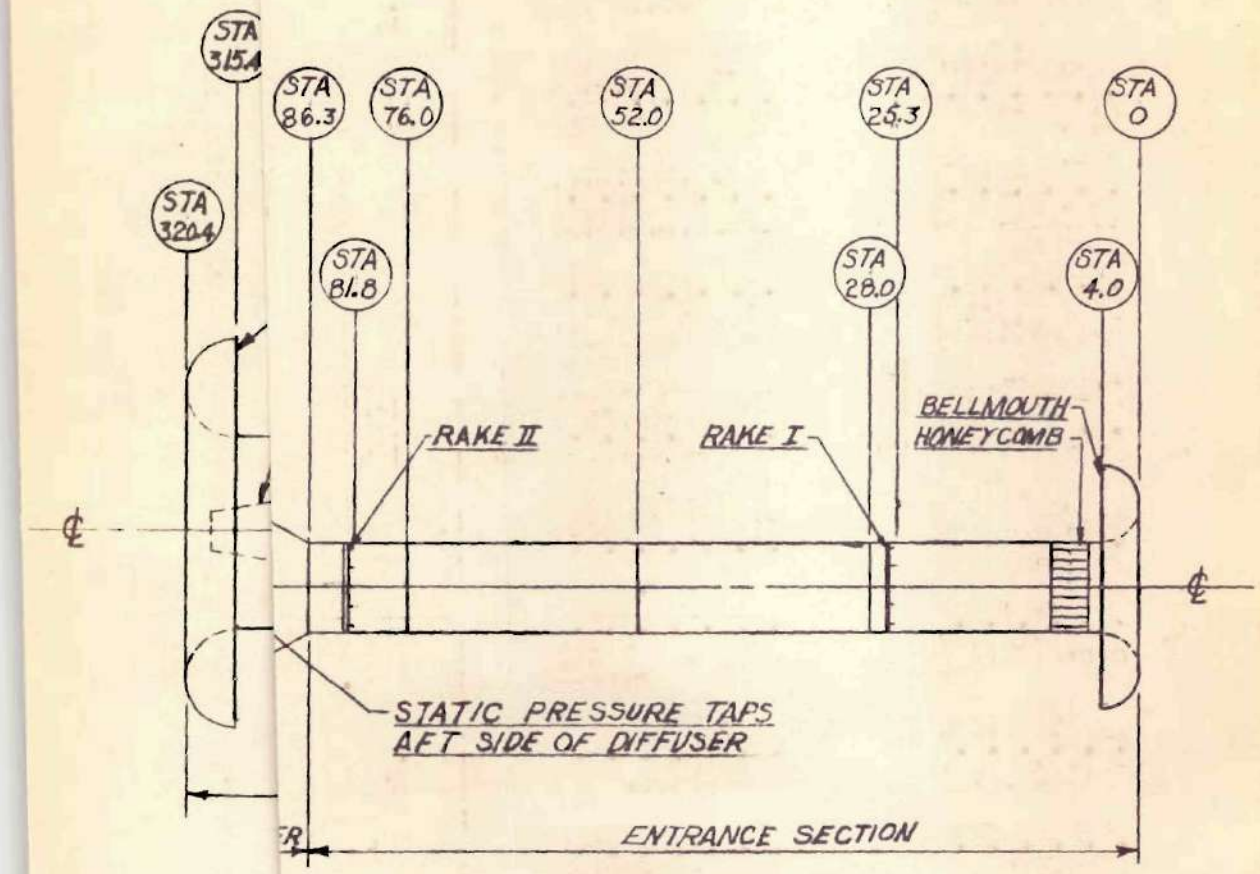
STA 315.4
STA 320.4
STA 86.3
STA 81.8
STA 76.0
STA 52.0
STA 25.3
STA 28.0
STA 0
STA 4.0
RAKE II
RAKE I
BELLMOUTH HONEYCOMB
STATIC PRESSURE TAPS AFT SIDE OF DIFFUSER
ENTRANCE SECTION

Fig. 2 Photograph of Wind Tunnel

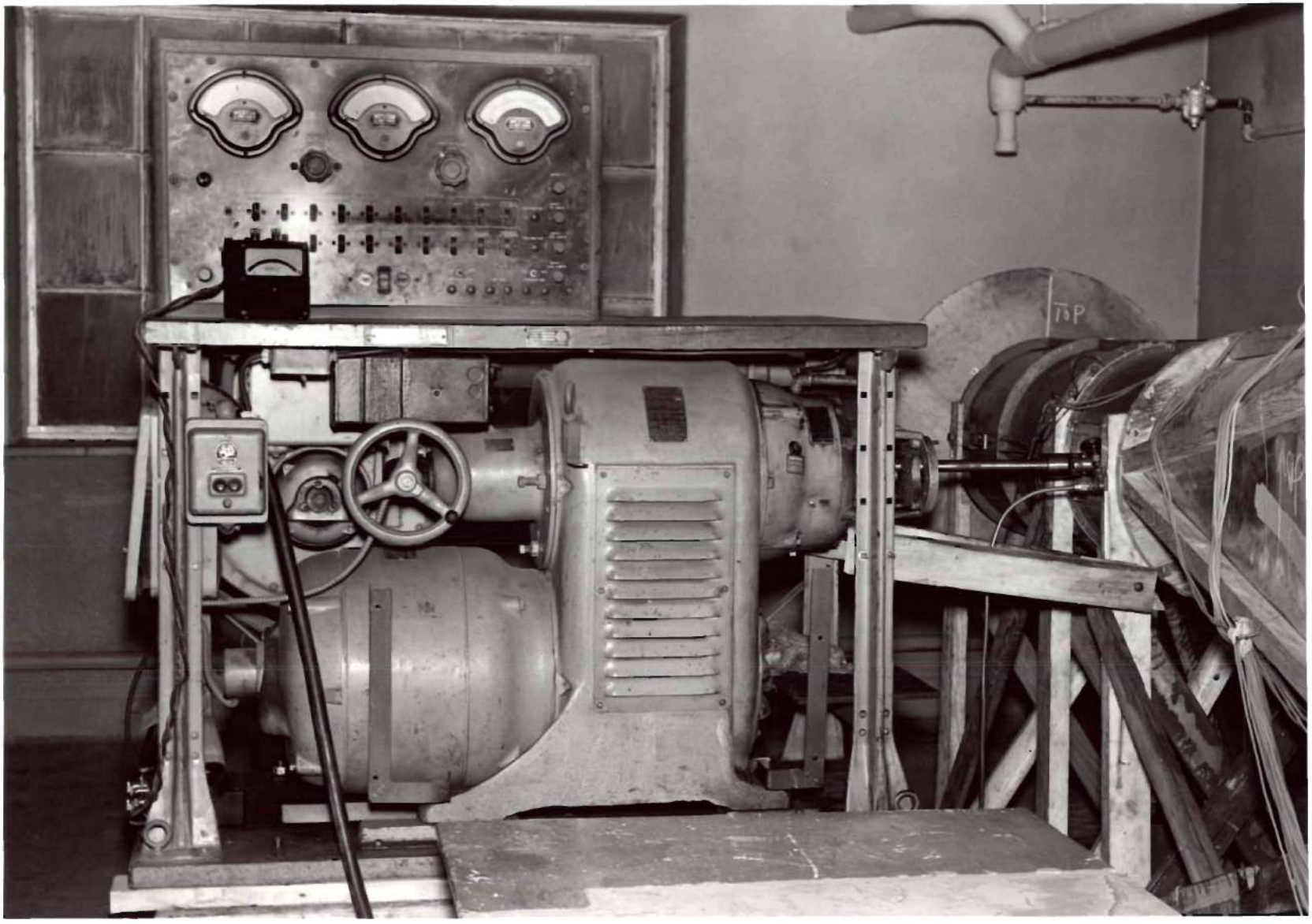

Fig. 3 Photograph of Power Supply

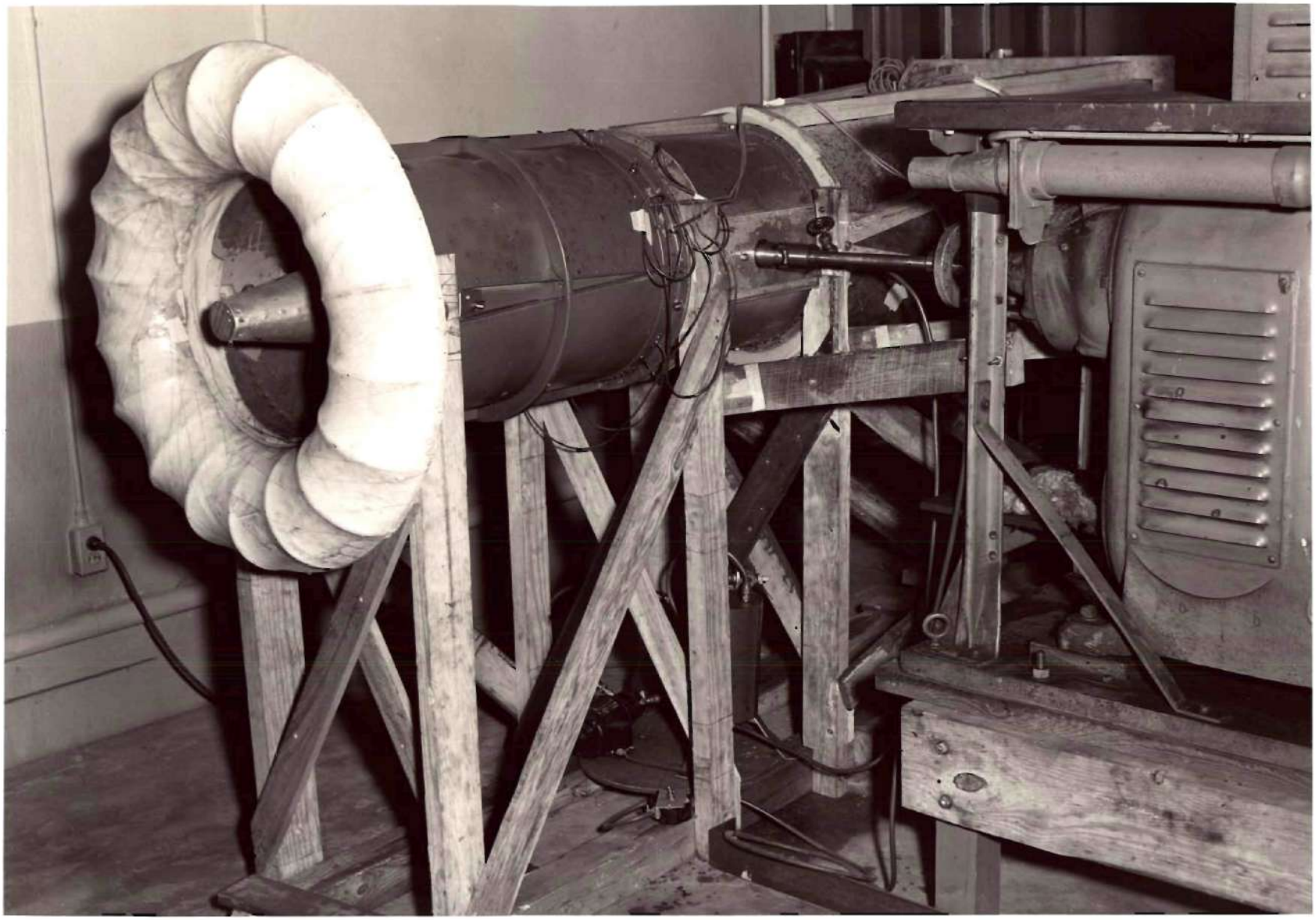

Fig. 4 Photograph of Exit Bell-mouth

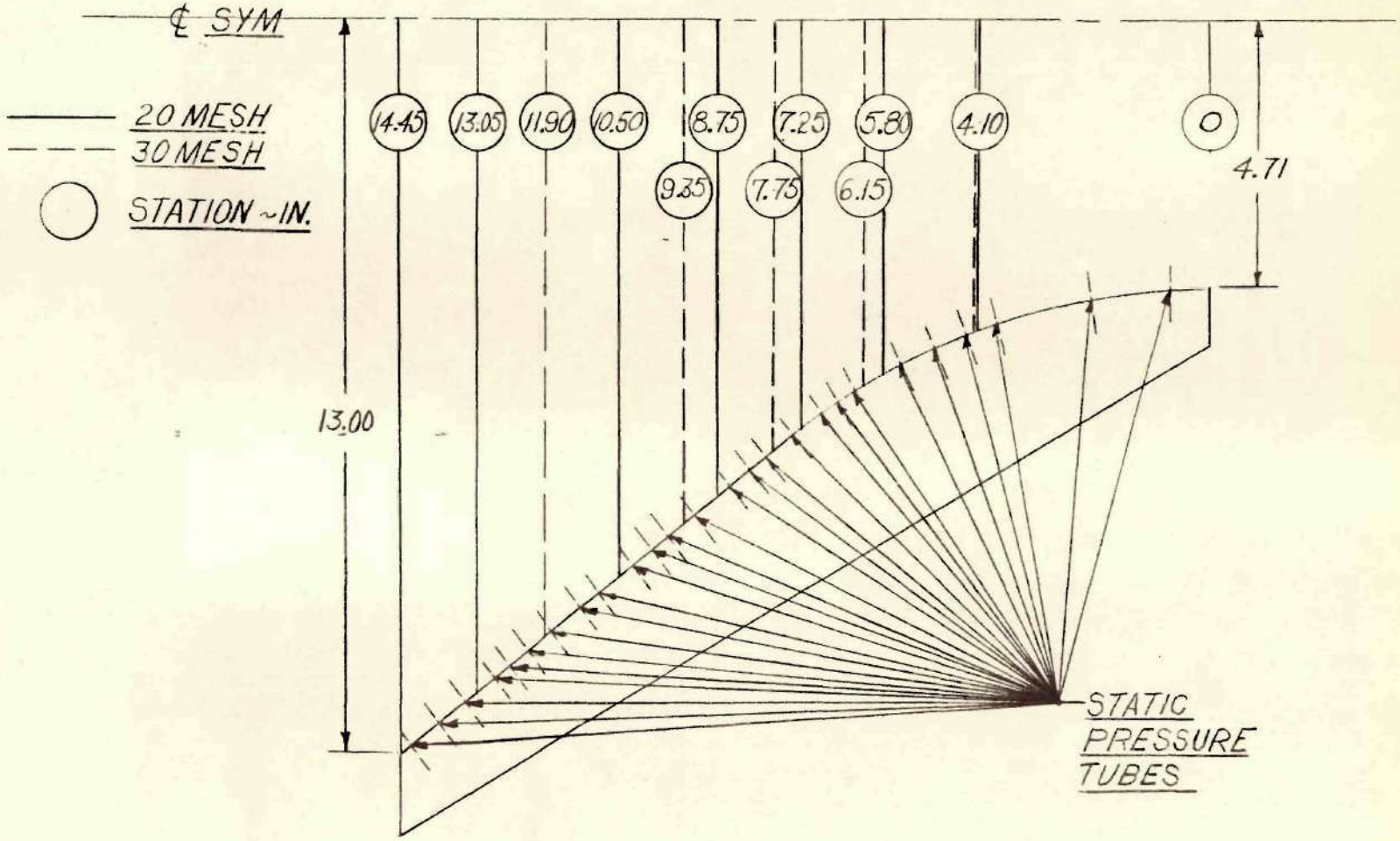

FIG. 5
DIFFUSER SCHEMATIC

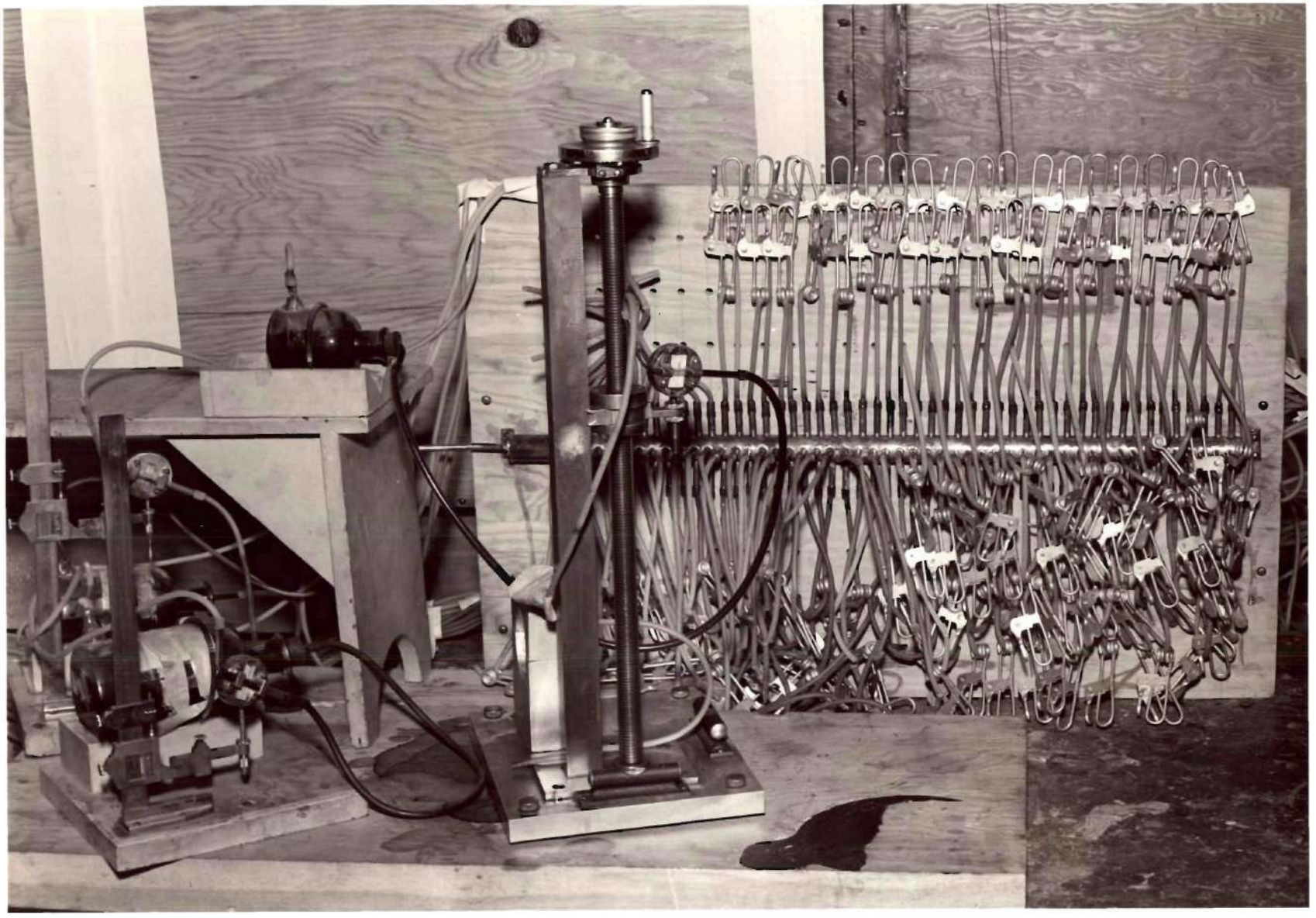

Fig. 6 Photograph of Pressure Manifold

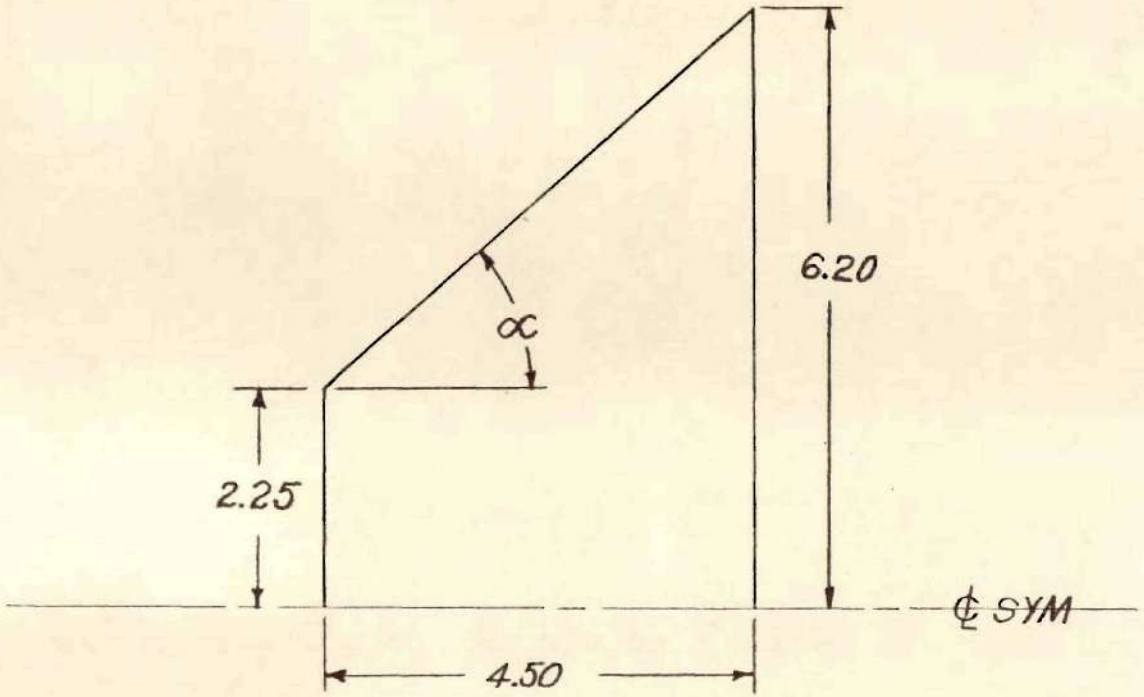

FIG. 7
BASIC DIFFUSER
GA. TECH LOW TURBULENCE
WIND TUNNEL

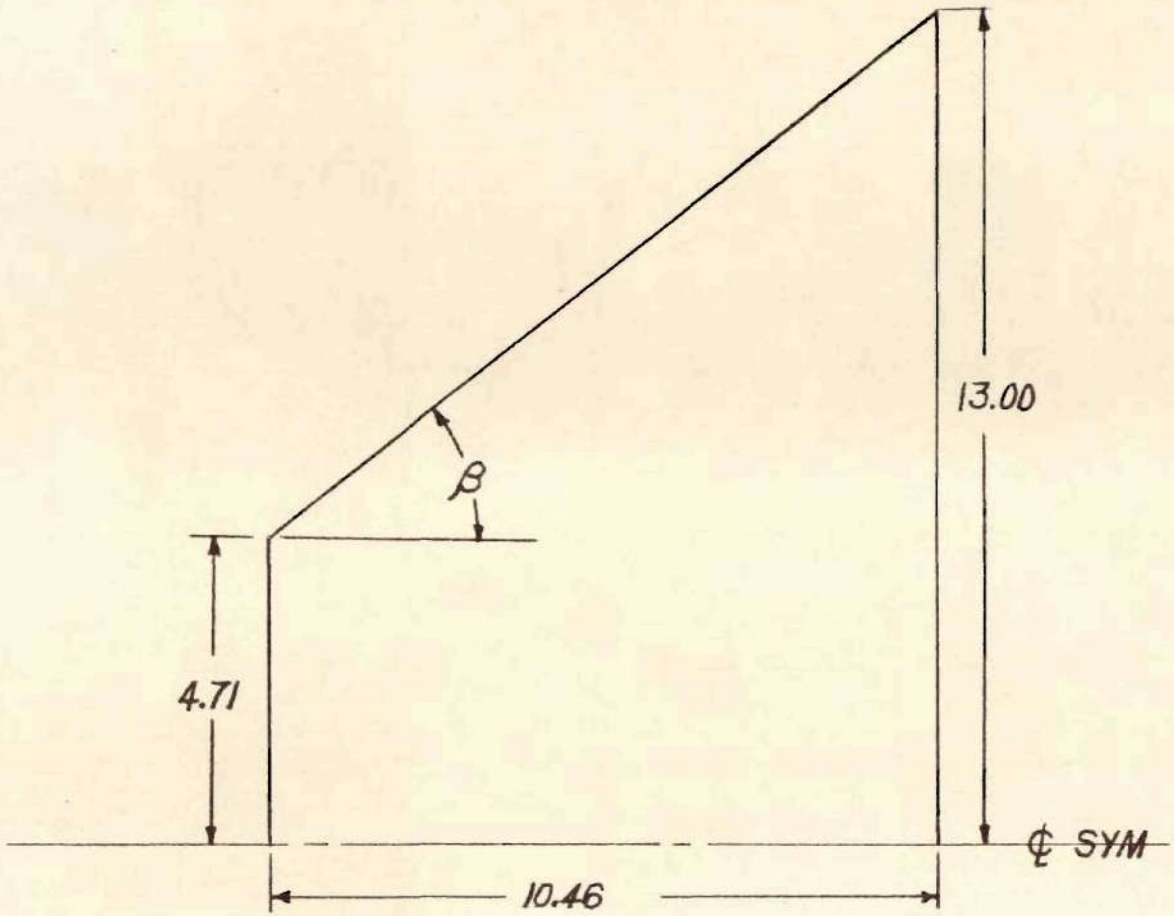

FIG. 8
BASIC DIFFUSER
MODEL

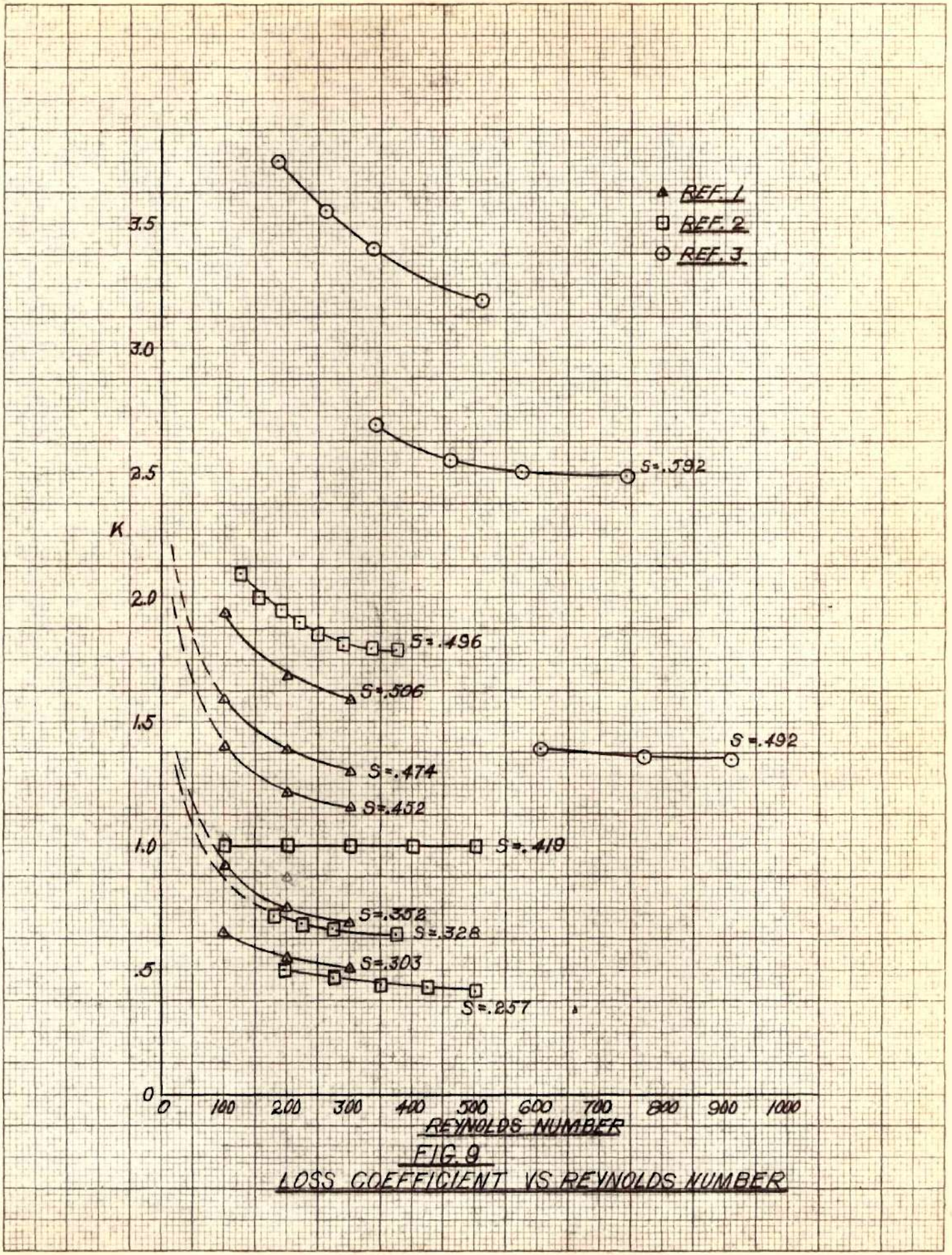

FIG. 9

LOSS COEFFICIENT VS REYNOLDS NUMBER

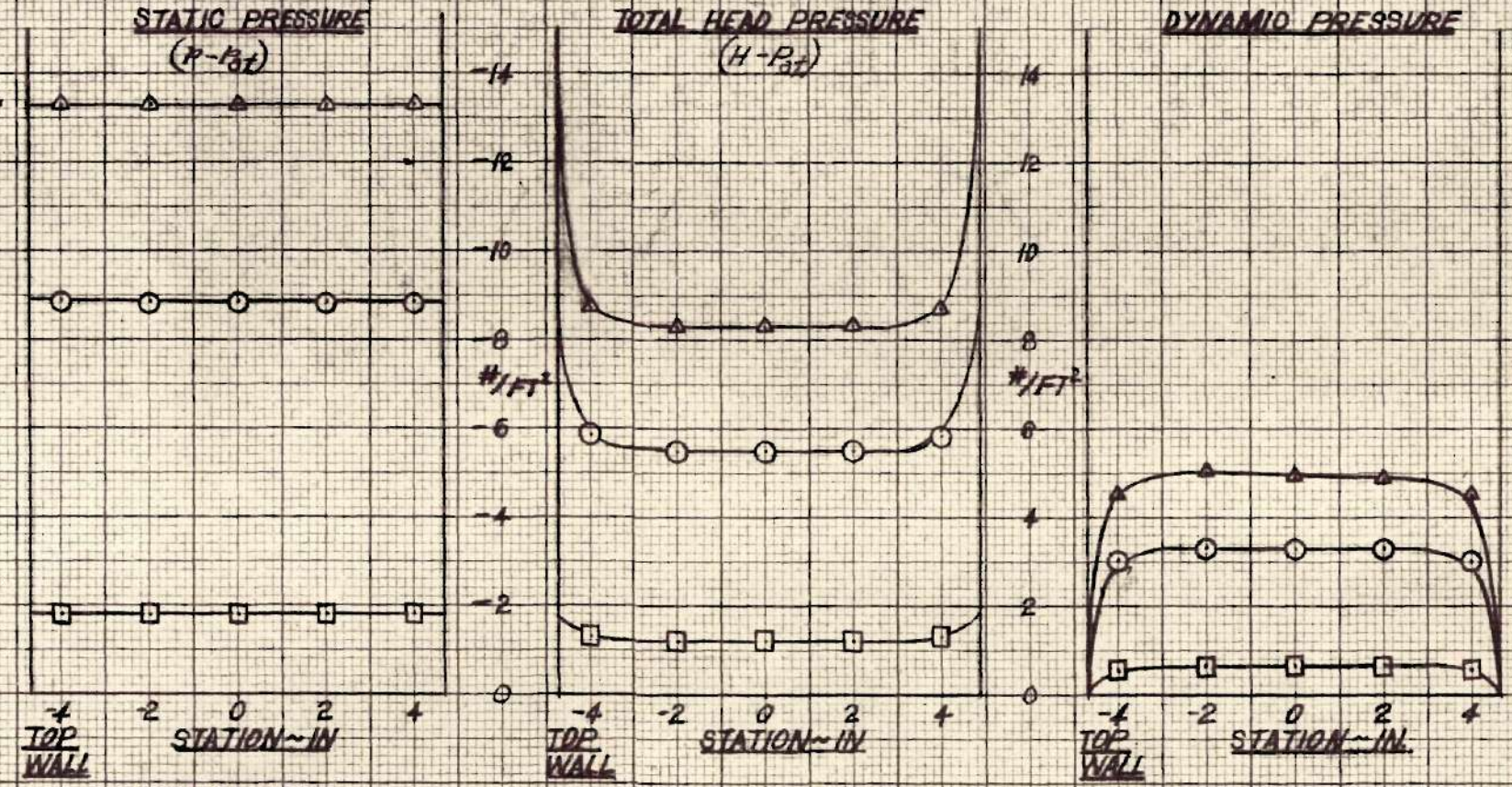

FIG. 10
RAKE II
20 X 20 MESH SCREENS
PRESSURE DISTRIBUTIONS

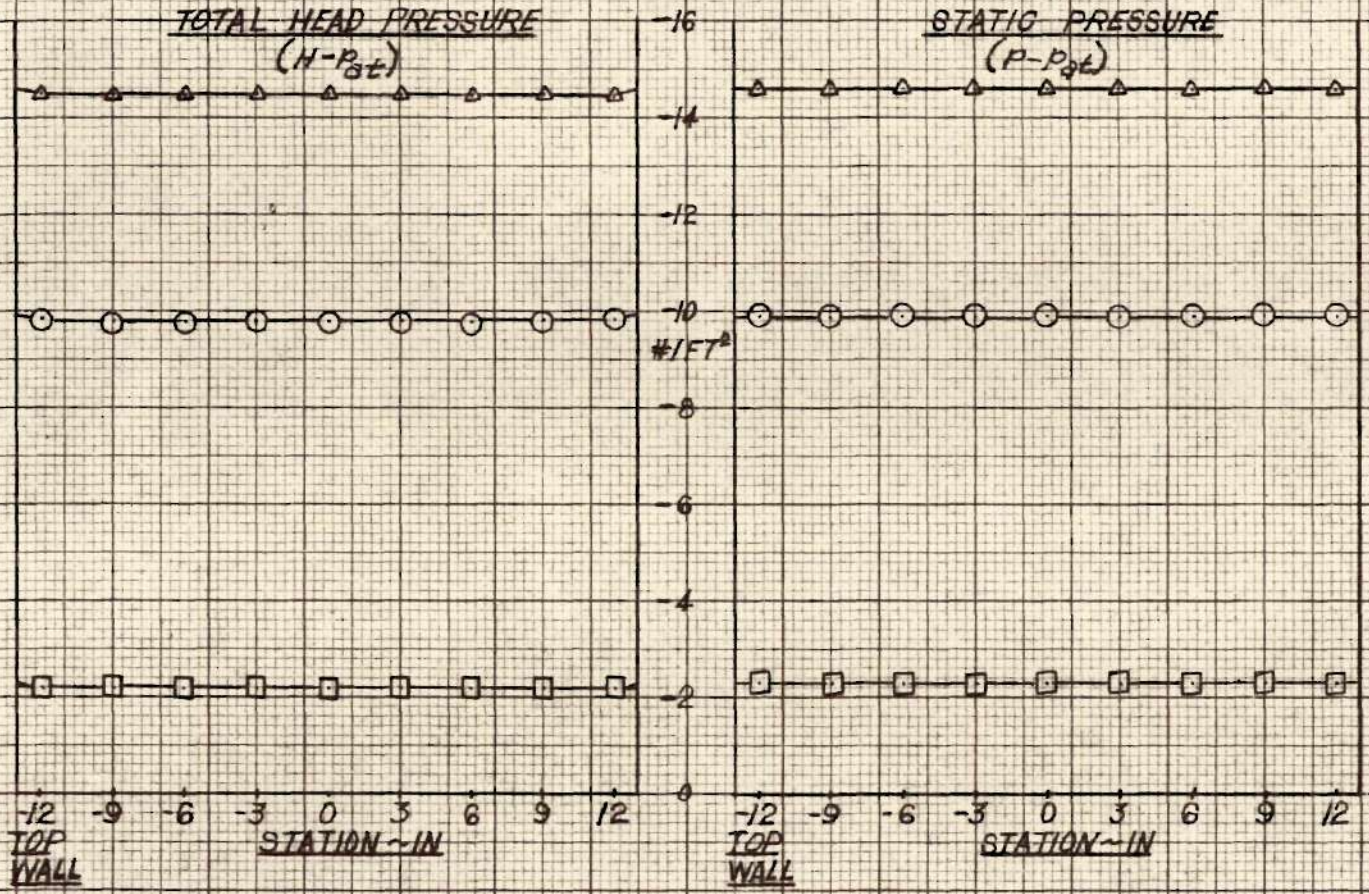

VELOCITIES AT DIFFUSER ENTRANCE
□ 22.7 FT/SEC.
○ 51.8 FT/SEC.
△ 62.4 FT/SEC

FIG. 11
RAKE III
20X20 MESH SCREENS
PRESSURE DISTRIBUTIONS

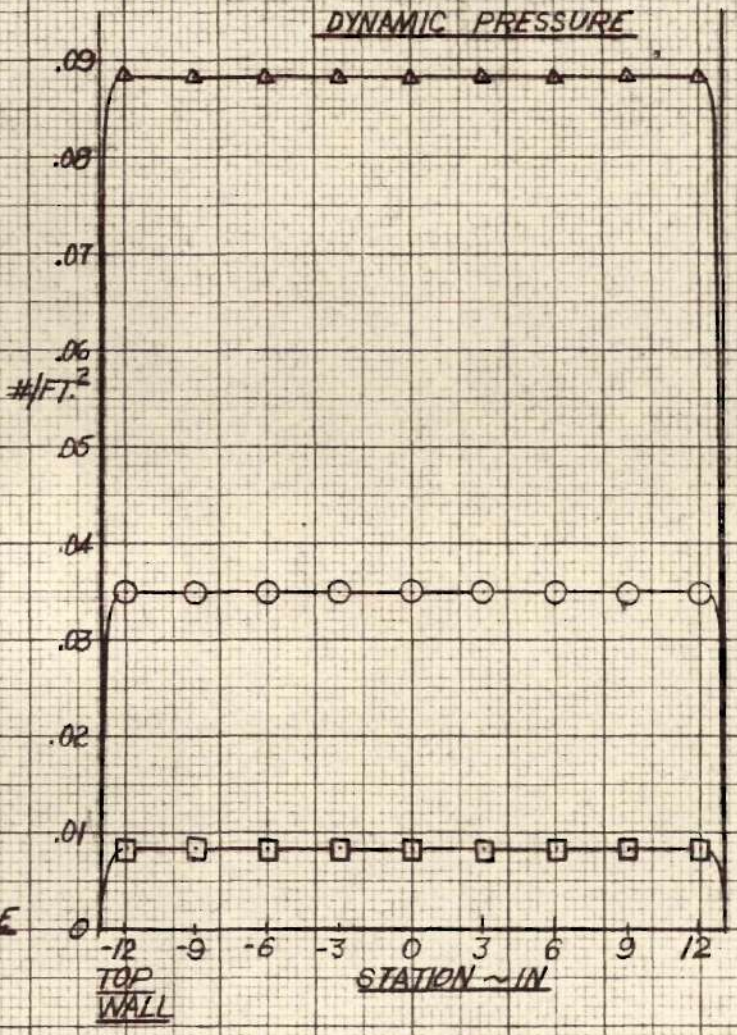

VELOCITIES AT DIFFUSER ENTRANCE
- ⊡ 22.7 FT/SEC.
- ⊙ 61.8 FT/SEC.
- ▲ 62.4 FT/SEC.

FIG.12
RAKE III
20X20 MESH SCREENS

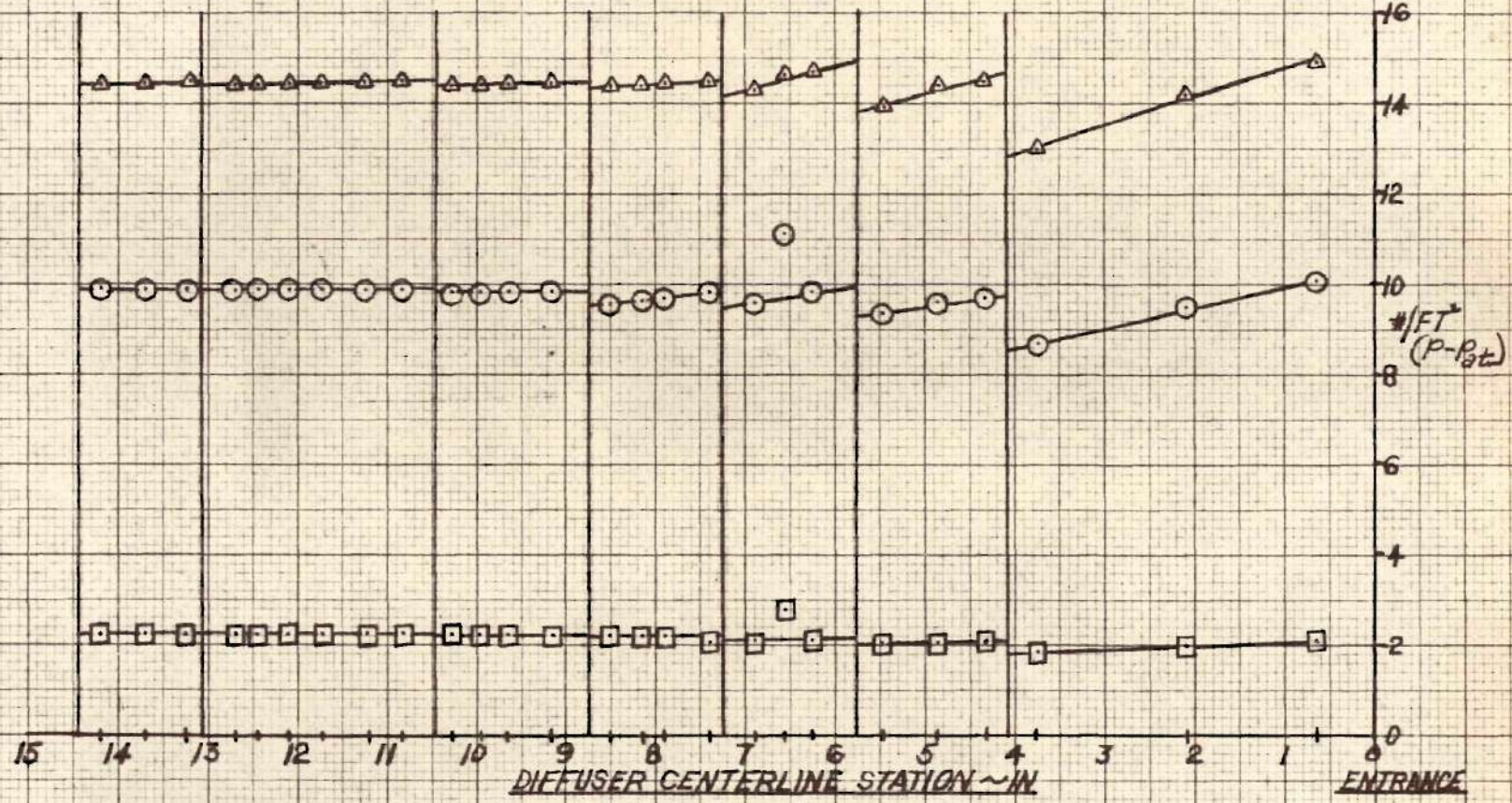

VELOCITIES AT DIFFUSER ENTRANCE
- ⊡ 22.7 FT/SEC
- ⊙ 51.8 FT/SEC
- ▲ 62.4 FT/SEC

FIG. 13
DIFFUSER STATIC PRESSURE AT WALL
20X20 MESH SCREENS

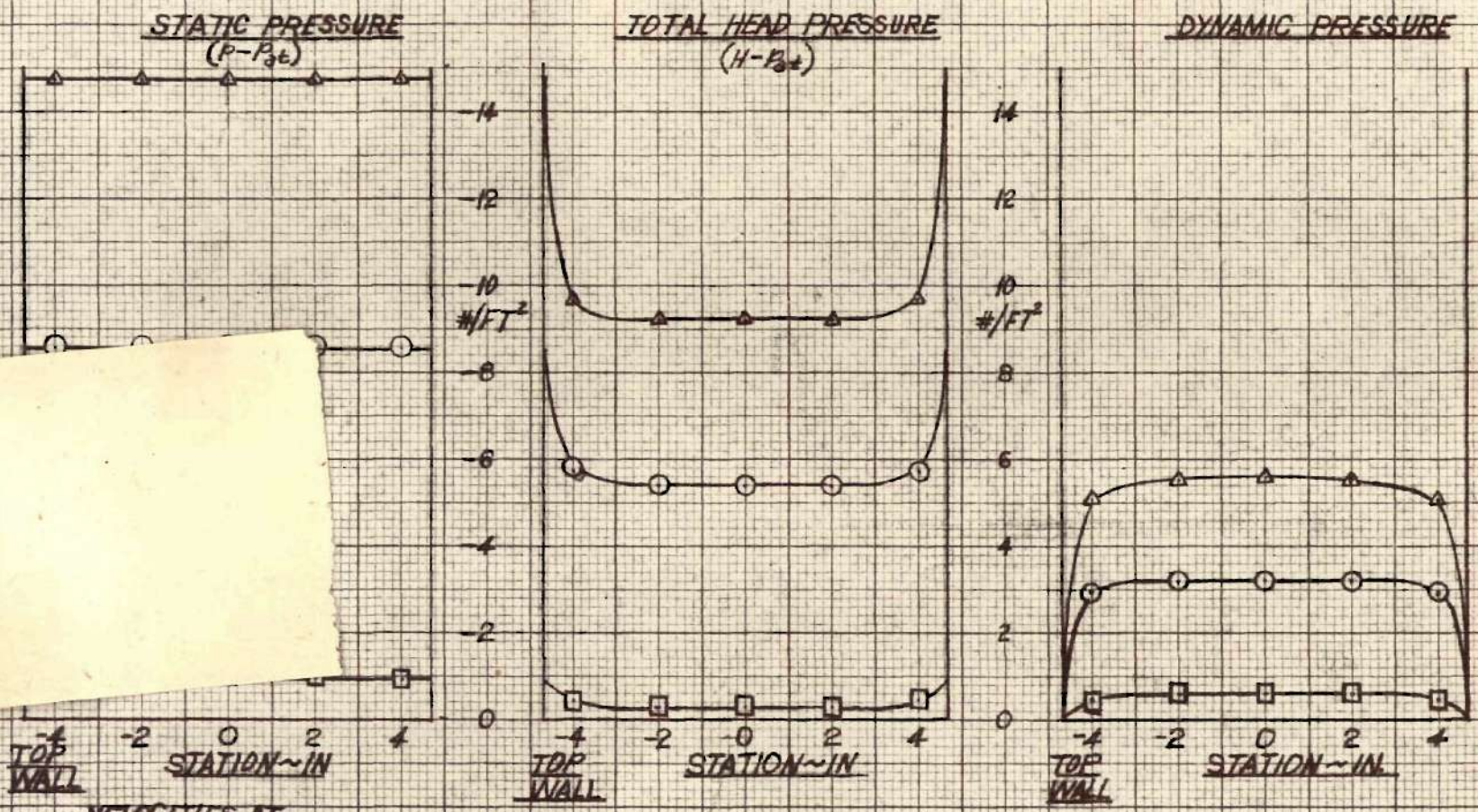

FIG. 14
RAKE II
30X30 MESH SCREENS
PRESSURE DISTRIBUTIONS

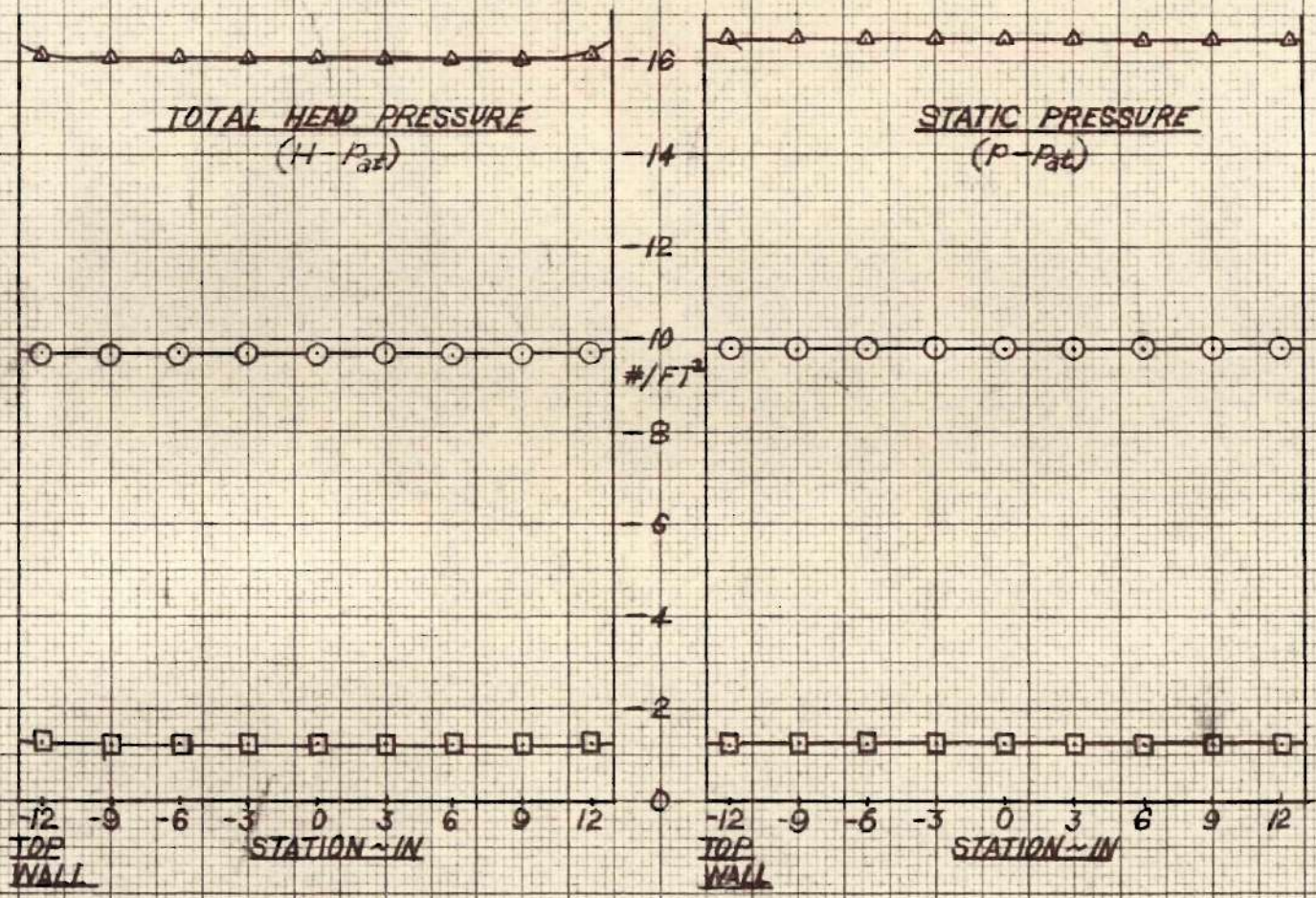

VELOCITIES AT DIFFUSER ENTRANCE

- ⊡ 21.2 FT/SEC.
- ⊙ 51.6 FT/SEC.
- ▲ 68.5 FT/SEC.

FIG. 15
RAKE III
30 X 30 MESH SCREENS
PRESSURE DISTRIBUTIONS

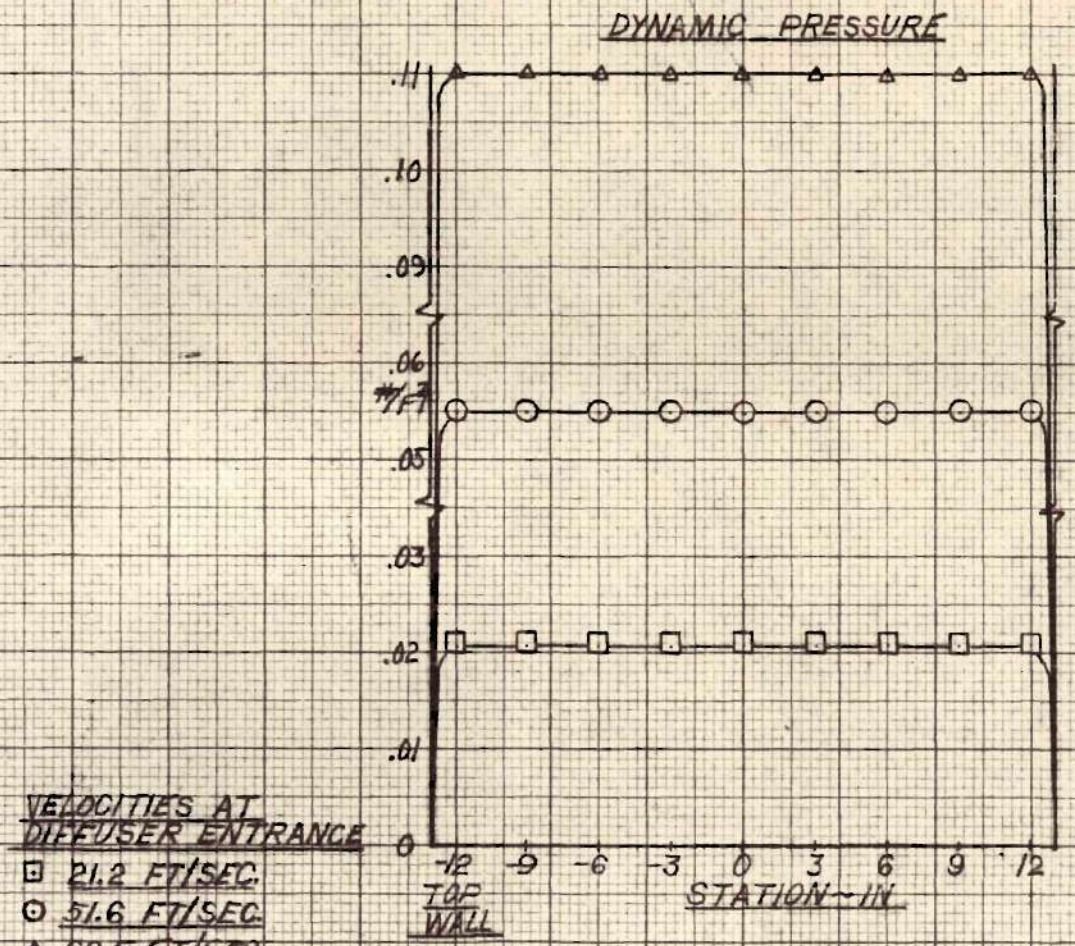

FIG. 16
RAKE III
30 X 30 MESH SCREENS

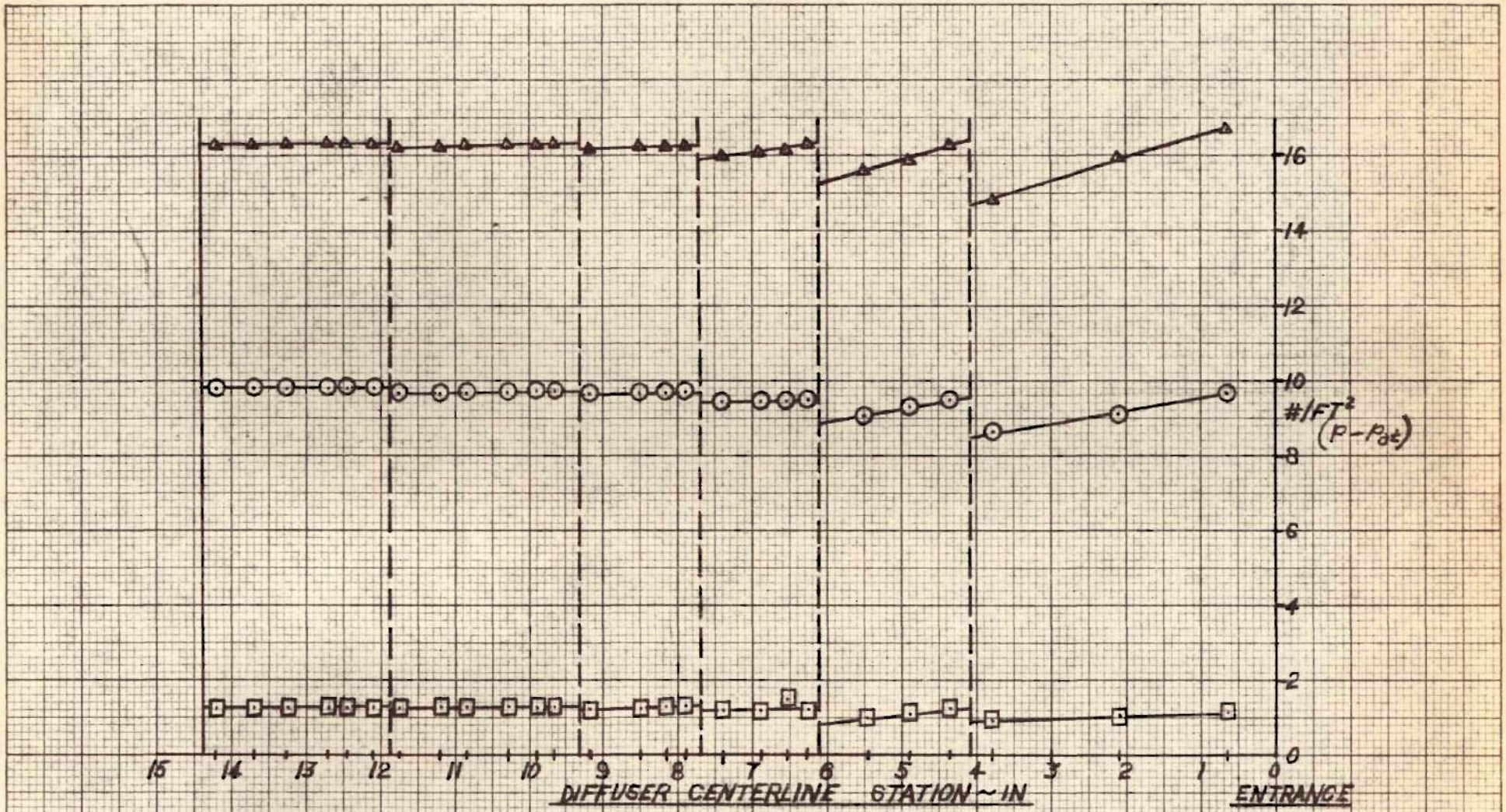

FIG. 17
DIFFUSER STATIC PRESSURE AT WALL
30 X 30 MESH SCREENS

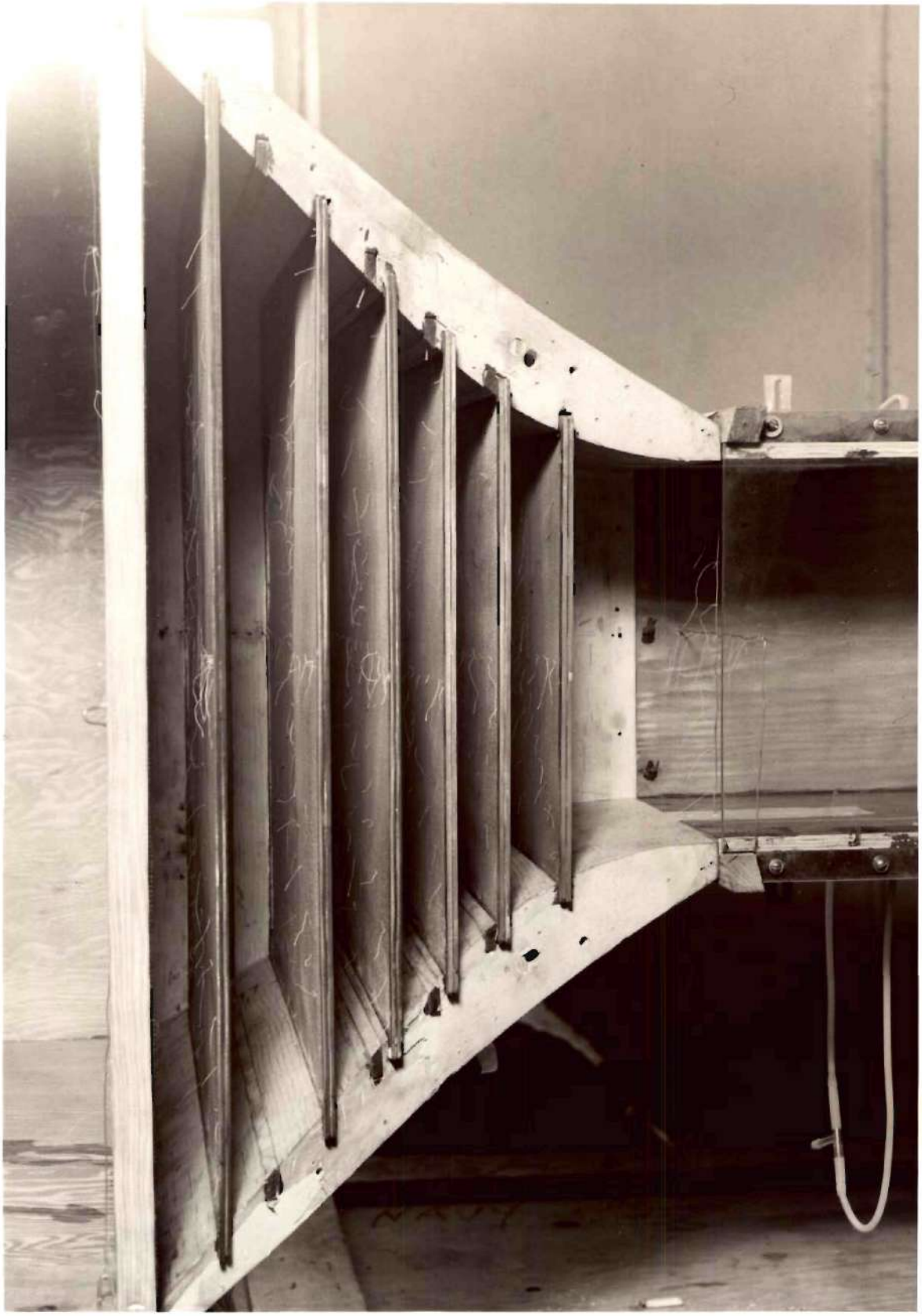

Fig. 18 Photograph of Diffuser with 20 x 20 Mesh Screens

Fig. 19 Tuft Study Upstream of Diffuser 20 x 20 Mesh Screens

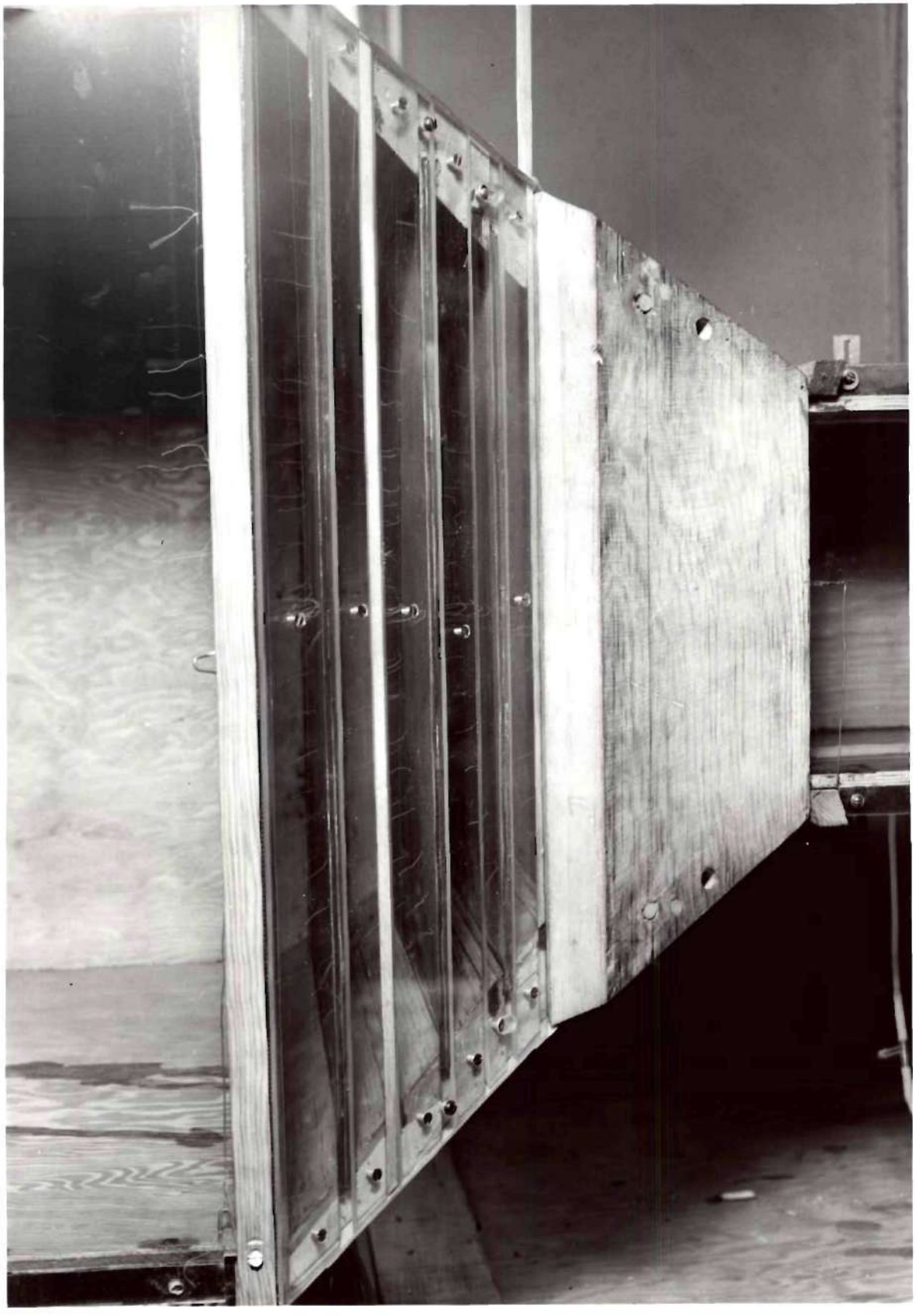

Fig. 20 Tuft Study in Diffuser 20 x 20 Mesh Screens

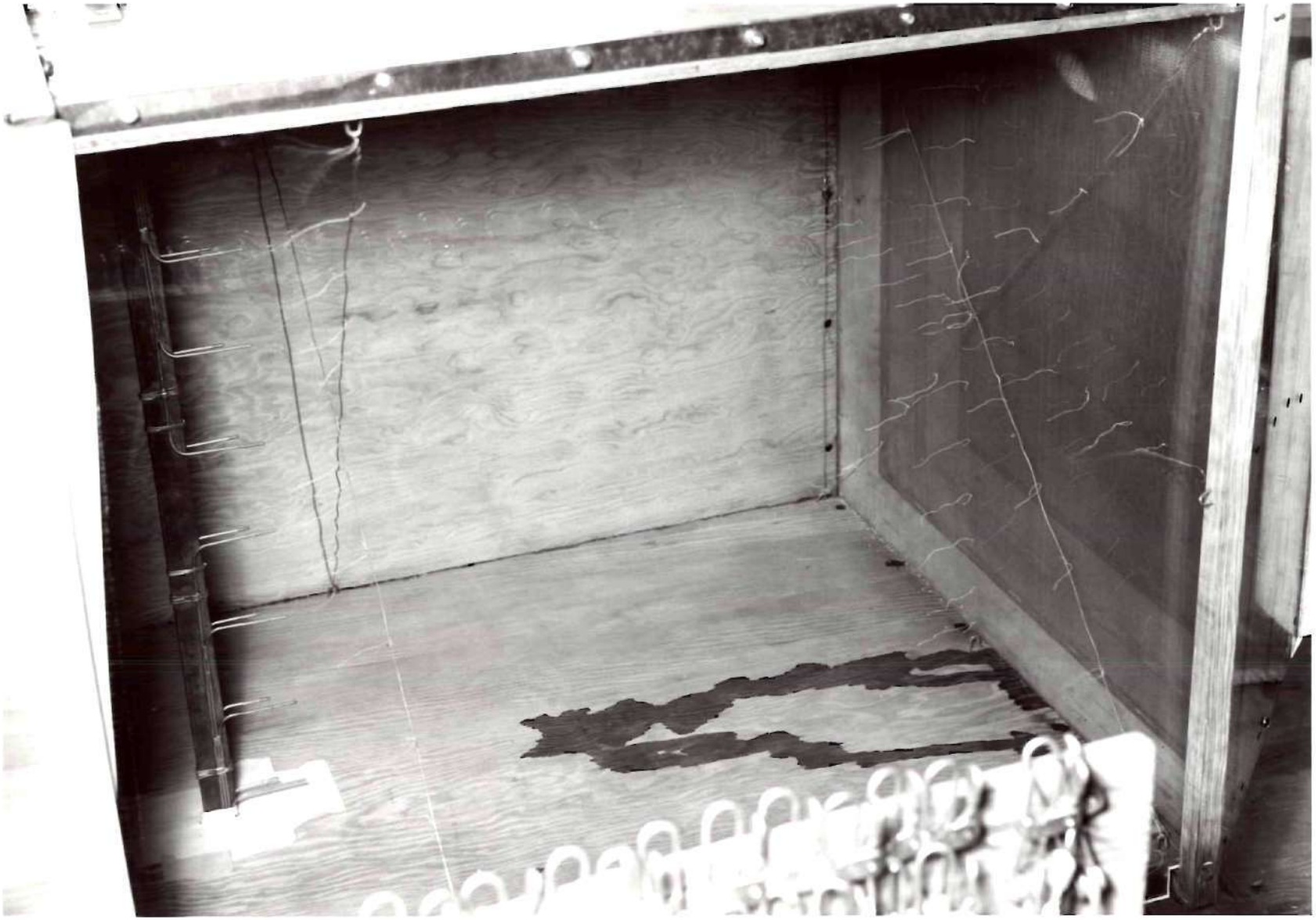

Fig. 21 Tuft Study Downstream of Diffuser 20 x 20 Mesh Screens

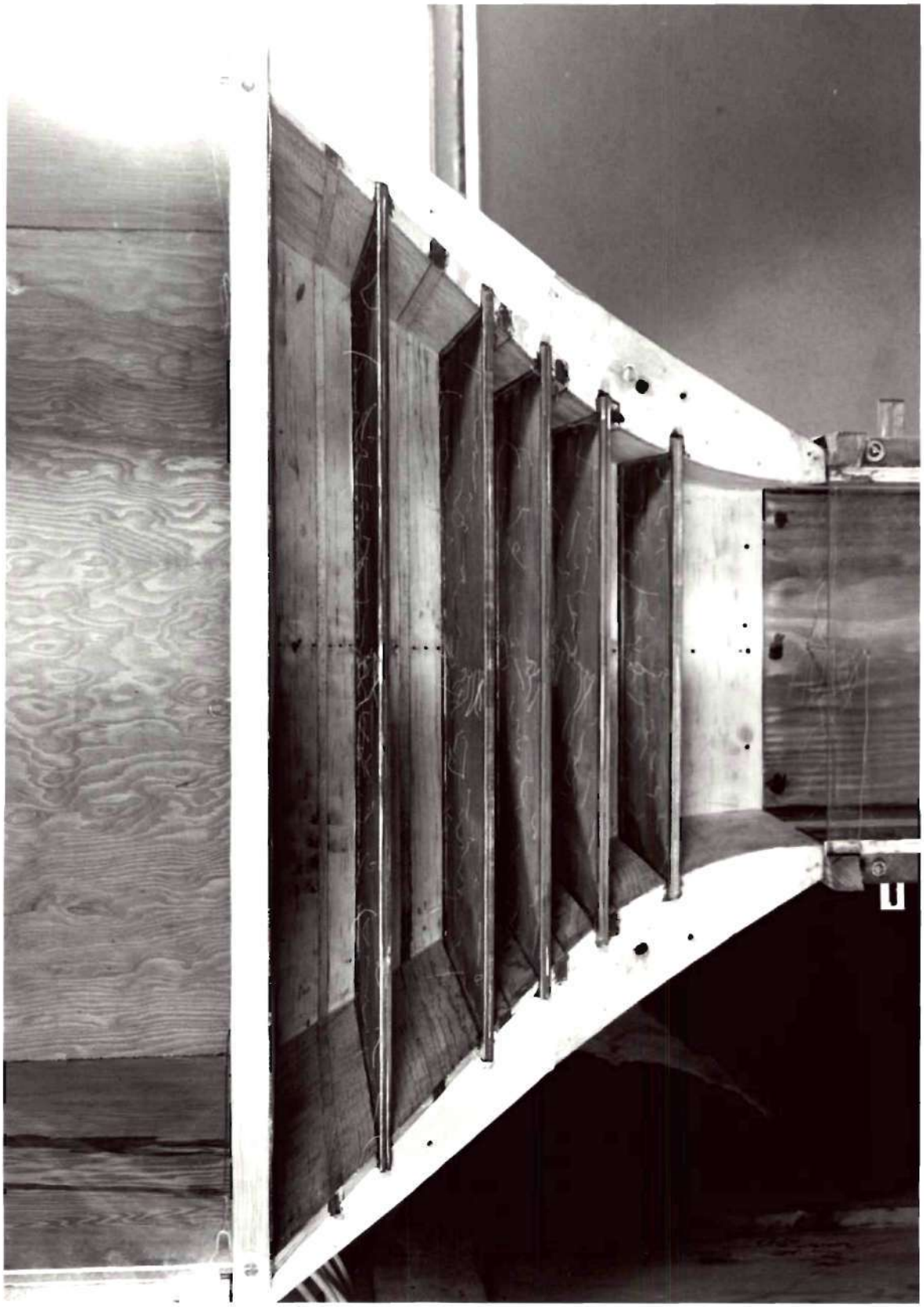

Fig. 22 Photograph of Diffuser with 30 x 30 Mesh Screens

Fig. 23 Tuft Study Upstream of Diffuser 30 x 30 Mesh Screens

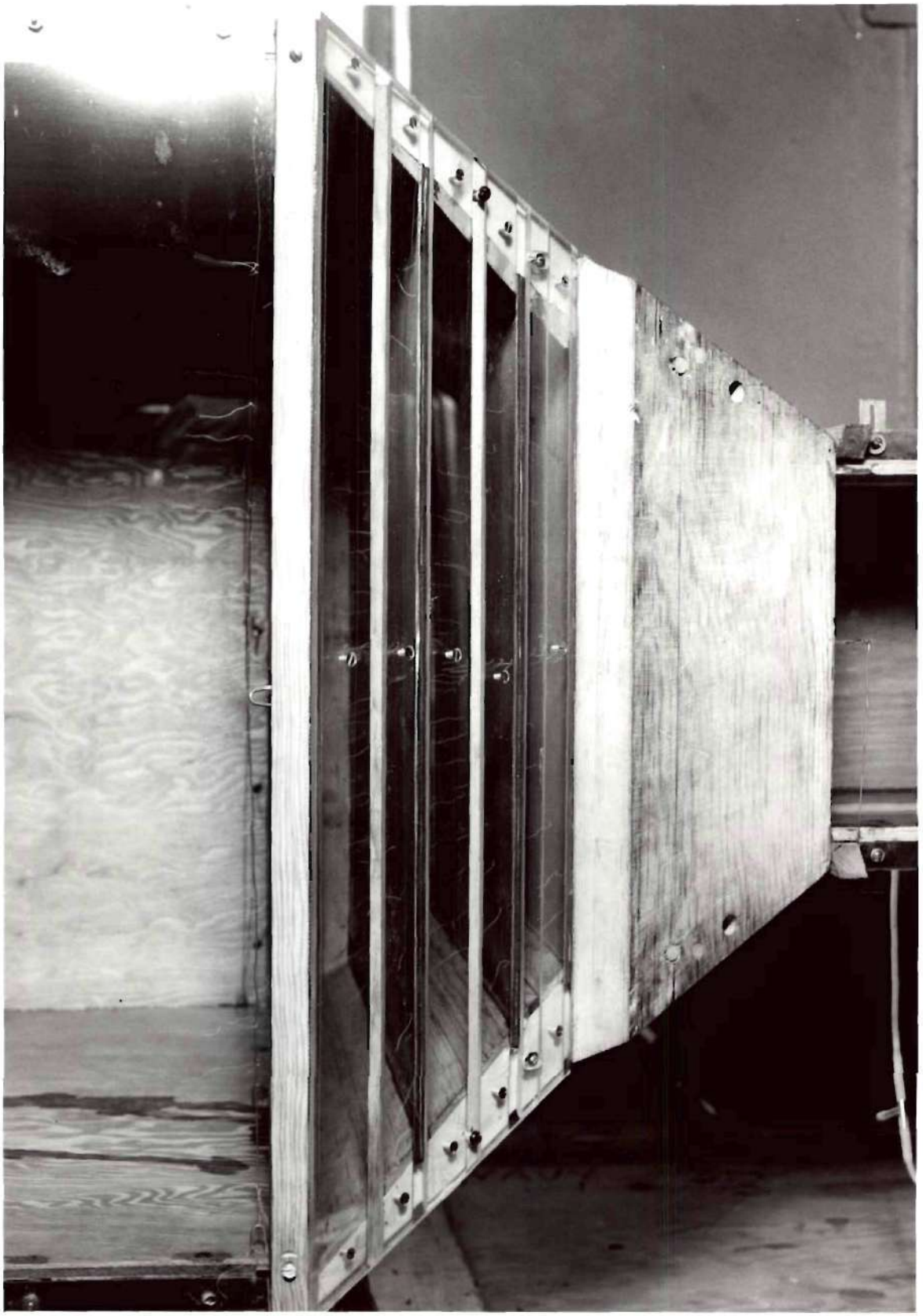

Fig. 24 Tuft Study in Diffuser 30 x 30 Mesh Screens

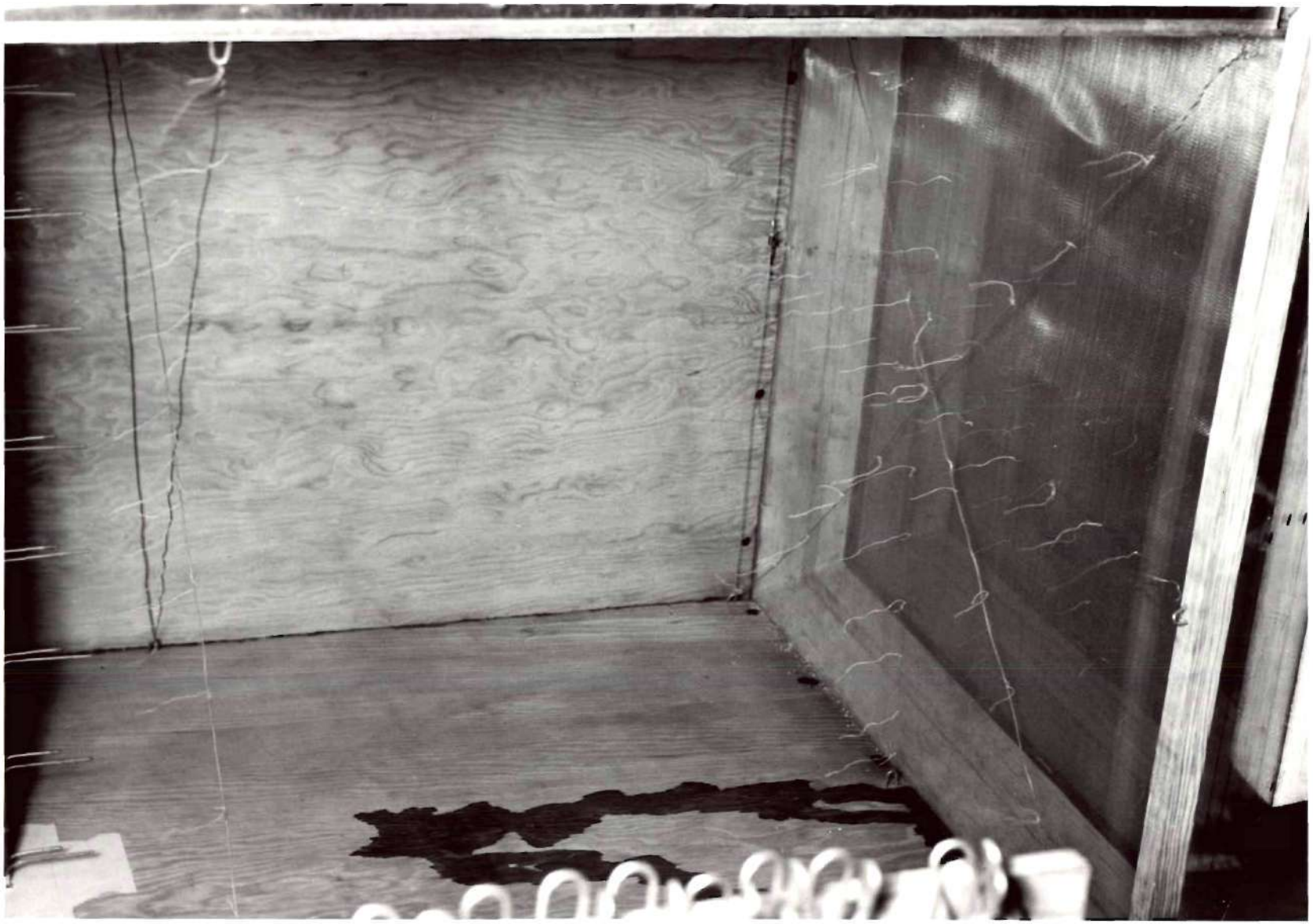

Fig. 25 Tuft Study Downstream of Diffuser 30 x 30 Mesh Screens

REFERENCES

1. Schubauer, G. B. and Spangenberg, W. G., Effect of Screens In Wide-Angle Diffusers; National Advisory Committee for Aeronautics, Technical Note No. 1610, Washington, July, 1948.

2. Eckert, B. and Pfluger, F., The Resistance Coefficient of Commercial Round Wire Grids, National Advisory Committee for Aeronautics, Technical Memorandum No. 1003, January, 1942.

3. Screen Resistance Coefficient Tests, United Aircraft Corporation, Res. Div. M-517, July, 1944.

PART II

THE INFLUENCE OF
THE PROXIMITY OF A WALL TO THE TEST SECTION
EXIT OF A WIND TUNNEL

SUMMARY

The purpose of this part of the paper is to present the results of tests made to determine the influence of the proximity of a wall to the test section exit on the velocity and static pressure distributions in the tunnel working section.

A blower and adjustable wall plane were installed to simulate the conditions for these tests. The duct was calibrated by use of static and total head pressure probes without the wall plane in position. Static and total head pressure measurements were made at the duct centerline at several axial locations in the vicinity of the duct exit while varying the wall plane location from one-half to five duct diameters from the exit for each of several velocities varying from 29.7 to 62.4 feet per second. Static and dynamic pressure distributions across the duct as close to the duct exit as possible were also made.

The results indicate that the effect on the centerline values of the static and dynamic pressures within the tube was negligible when the wall was located at a distance greater than one tube diameter from the exit of the duct. The effect on the static and dynamic pressure distributions within the tube was found to be negligible also for wall locations greater than one tube diameter from the duct.

LIST OF SYMBOLS

S_0	Pitot tube located 2.25 inches inside of exit
S_1	Pitot tube located 6.0 inches inside of exit
S_2	Static tube located 12.0 inches inside of exit
S_3	Static tube located 18.0 inches inside of exit

CHAPTER I

INTRODUCTION

The purpose of this part of the paper is to present the results of tests made to determine the influence of the proximity of a wall to the test section exit on the velocity and static pressure distributions in the tunnel working section.

Because of space limitations encountered in the design of the low turbulence wind tunnel at the Georgia Institute of Technology, it was found necessary to determine the magnitude of the aforementioned wall interference.

A literature search on the subject yielded very little pertinent information. Thus it was deemed essential to conduct these tests before the low turbulence wind tunnel design was completed.

CHAPTER II

INSTRUMENTATION AND EQUIPMENT

The airstream was supplied by a Buffalo Forge Blower, Number 5E, manufactured by the Buffalo Forge Company, Buffalo, New York, and powered by a 5 H.P. Sterling "Cros-Line" Motor, type KF, manufactured by Sterling Electric Motors, Inc., Los Angeles, California.

The mass flow of the blower was controlled by a throttle valve which was a conical block of wood attached to a threaded shaft in such a manner that turning the block would cause the block to advance toward the inlet of the blower and thereby decrease the inlet area and volume flow through the blower.

After leaving the blower the air passed through a five inch diameter steel tube fifty inches long, and then against a wall plane placed at various tube diameters from the exit of the tube. A schematic layout of the apparatus is shown in Fig. 25.

CHAPTER III

PROCEDURE

Before any pressure measurements could be taken, it was necessary to calibrate the duct. This was accomplished by varying the mass flow through the blower and reading the difference in total head and static pressure in the tube, i.e. the dynamic pressure. This calibration was carried out without the wall plane.

The wall plane distance from the exit of the working section was varied from one-half to five tube diameters for each of several velocities varying from 29.7 to 62.4 feet per second while the total head and static pressure measurements were recorded for each position and speed.

Since the influence of the wall plane would be most critical at the duct exit the static and dynamic pressure surveys across the tube were made as close to the duct exit as possible. For practical reasons this station was selected at 2.25 inches inside the duct exit.

These tests were conducted in two parts, (a) the effect of the proximity of the wall plane on the axial static and dynamic centerline pressures and (b) the effect of the wall plane on the radial static and dynamic pressure distributions 2.25 inches inside of the exit of the duct. a) In Figs. 27 through 29 the wall effect on the centerline static and dynamic pressures is shown. From these figures it can be seen that the interference effect is negligible for wall positions greater than one tube diameter from the exit for the range of velocities tested. When

the wall is located closer than one diameter to the exit the static pressure increases and the dynamic pressure decreases. This is to be expected as theoretically at a wall location of zero diameters the static and total head pressures should be equal and the dynamic pressure would be zero.

b) As seen in Fig. 30 the static and dynamic pressure distributions were essentially unaffected until the wall location was within one diameter of the exit. The percentage change in the value of the dynamic pressure with speed appeared to be approximately constant.

The data in Fig. 30 was rechecked and the scatter in points is attributed to instrument error.

CHAPTER IV

CONCLUSIONS

1) The effect on the centerline values of the static and dynamic pressures within the tube was found to be negligible when the wall was located at a distance greater than one tube diameter from the exit, for all speeds tested.

2) The effect on the static and dynamic pressure distribution within the tube was found to be negligible when the wall was located at a distance greater than one exit diameter, for all speeds tested.

CHAPTER V

RECOMMENDATIONS

In the design of Eiffel type tunnels where space limitations must be considered it is recommended that the tunnel exit be located at least one exit diameter from the wall plane. An alternate solution would require that no measurements be made in the vicinity of the duct exit in the presence of the wall plane unless interference corrections are made.

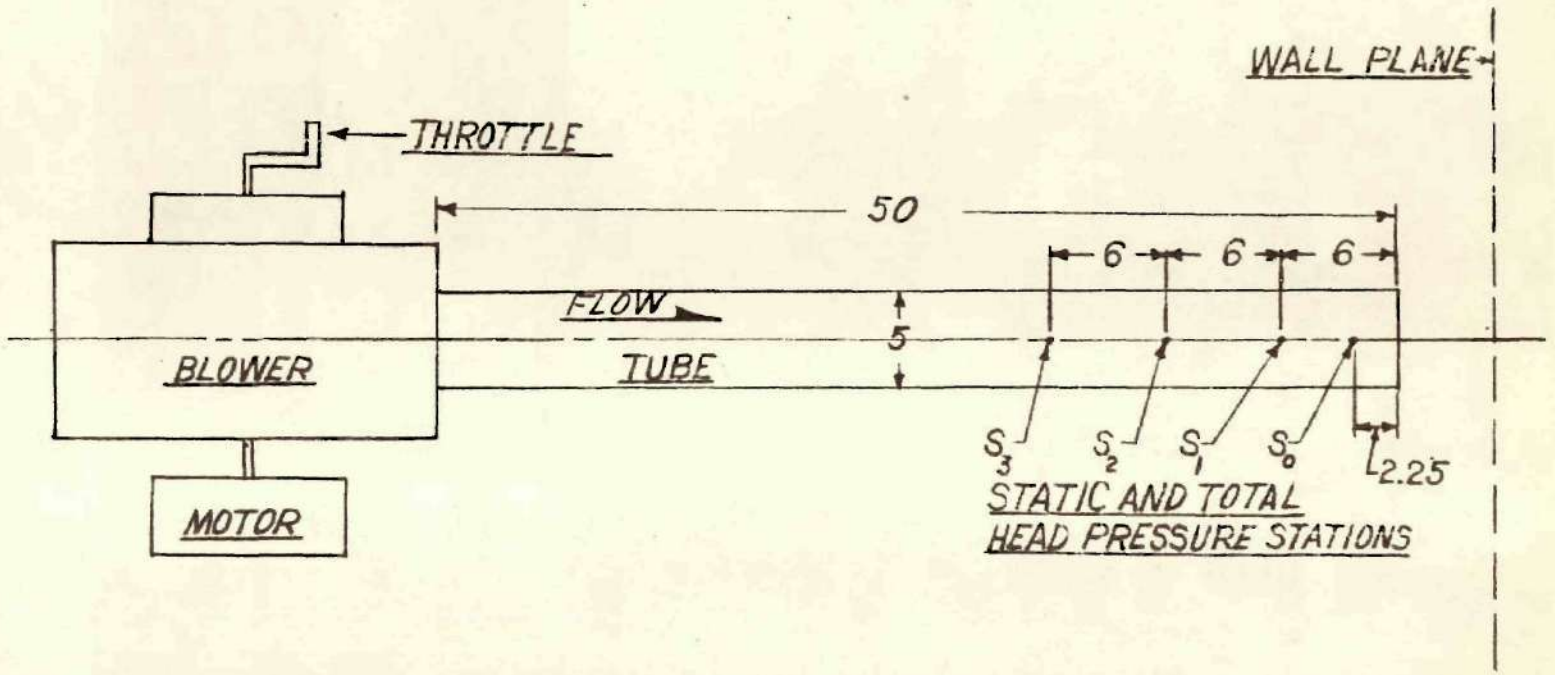

FIG. 26
SCHEMATIC OF APPARATUS

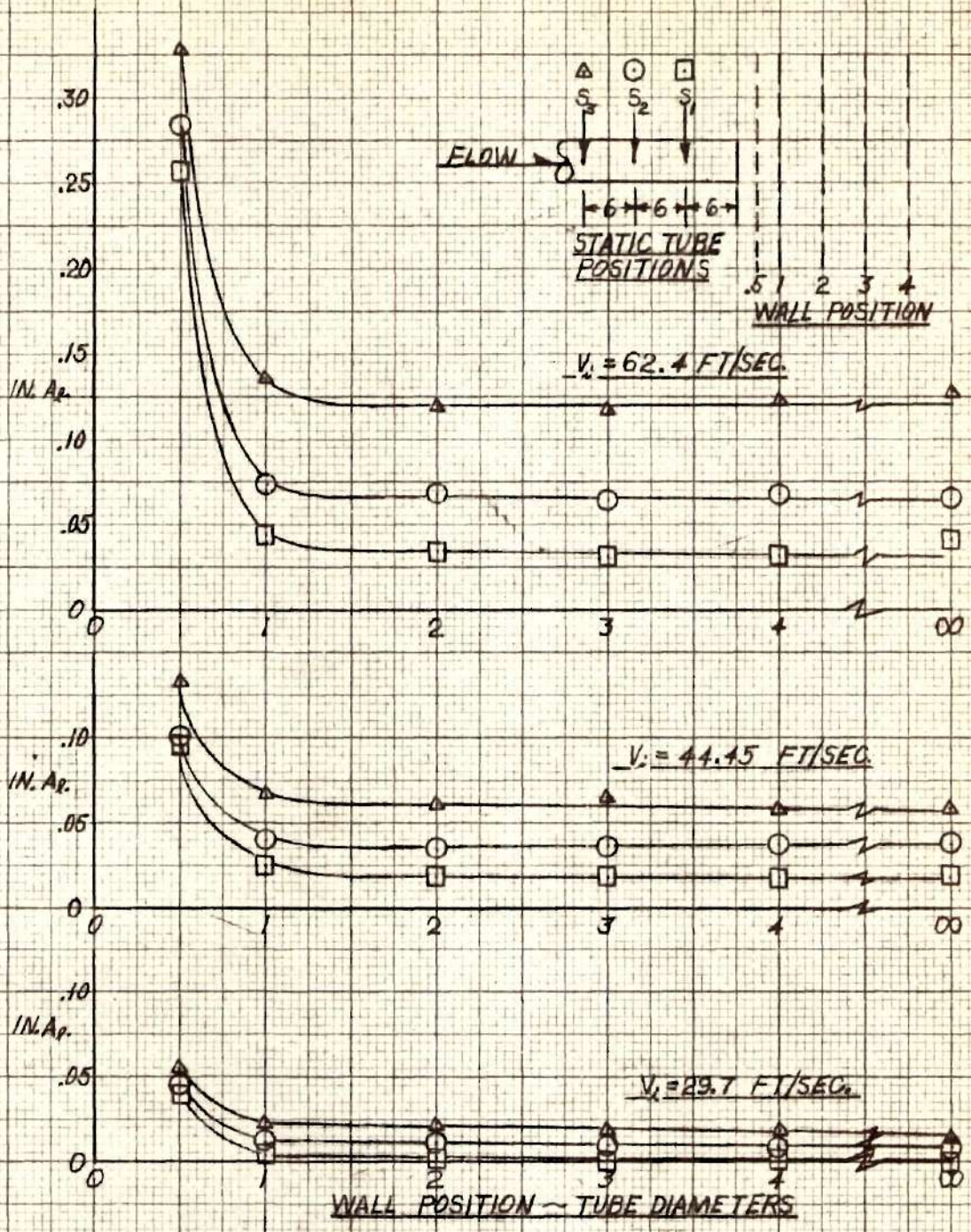

FIG. 27

VARIATION OF ℄ AXIAL STATIC PRESSURES WITH WALL PLANE LOCATION. (STATIONS S_1, S_2, S_3)

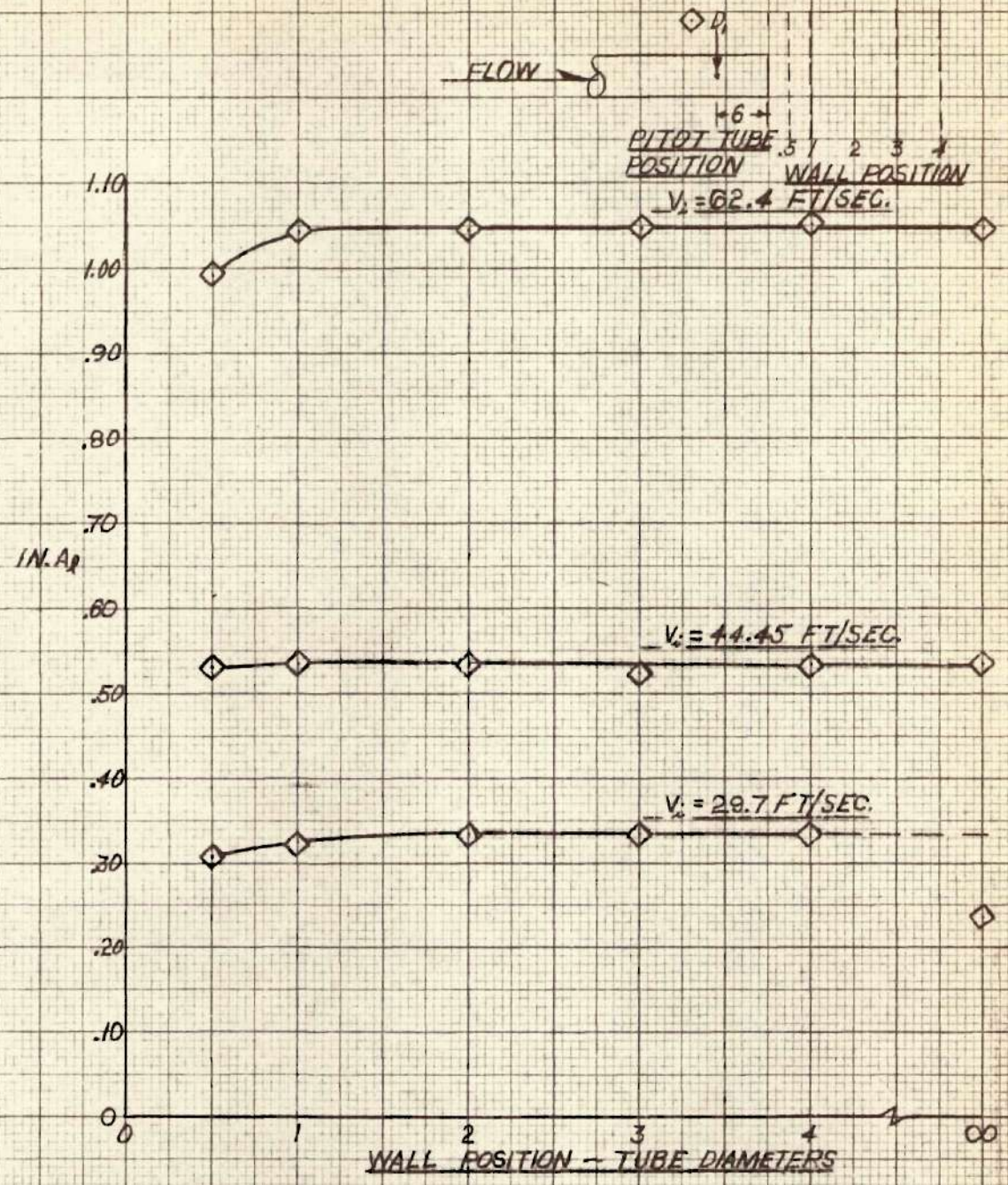

FIG. 28
VARIATION OF C_p DYNAMIC PRESSURE WITH WALL PLANE LOCATION (STATION D_1)

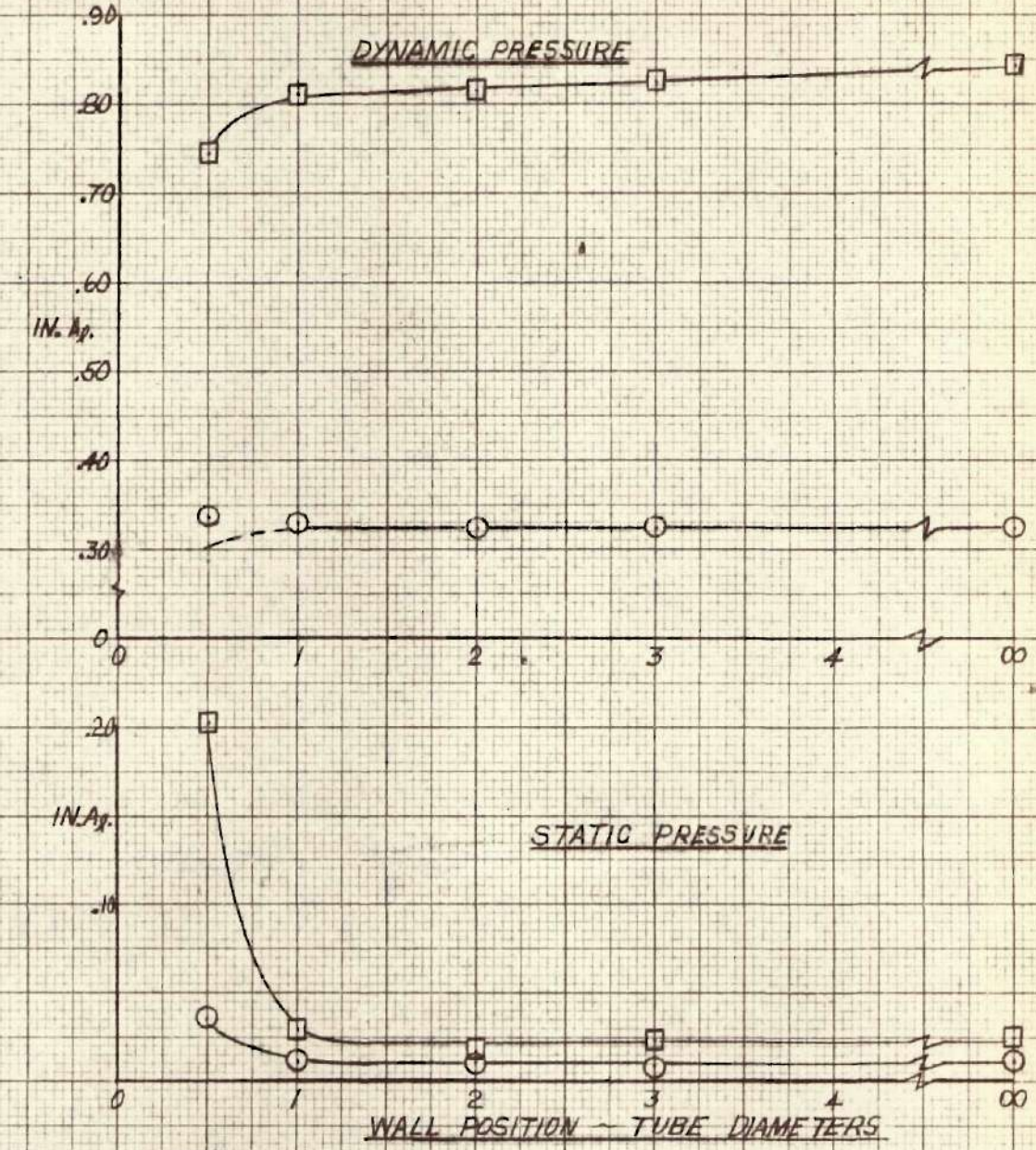

FIG. 29
VARIATION OF STATIC AND DYNAMIC ℄ PRESSURES WITH WALL PLANE LOCATION. (STATION S_0)

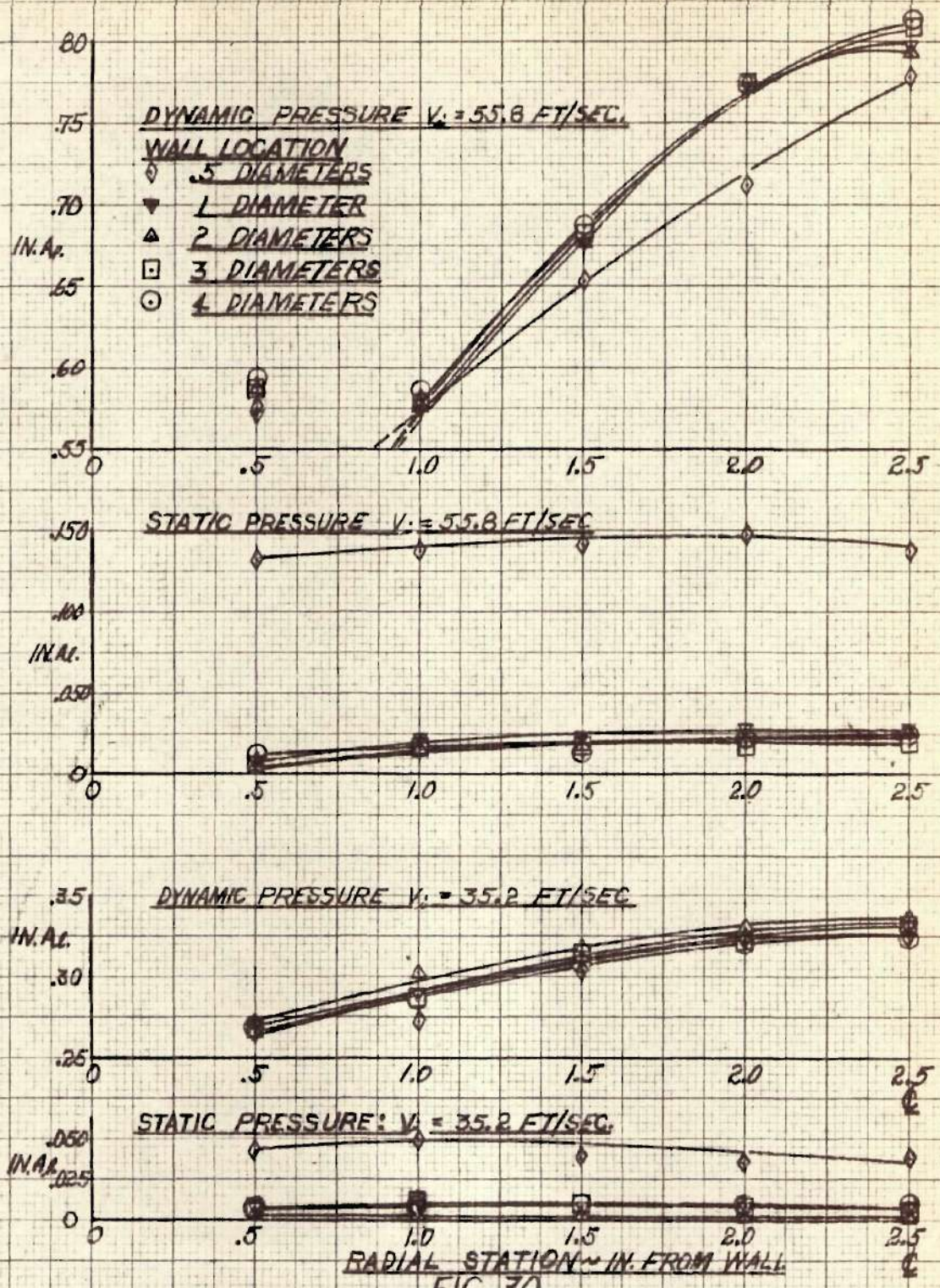

FIG. 30

RADIAL STATIC AND DYNAMIC PRESSURE DISTRIBUTIONS AS A FUNCTION OF WALL PLANE LOCATION. (STATION S_0)